UNIVERSIDADE TÉCNICA DO ATLÂNTICO
INSTITUTO DE ENGENHARIAS E CIÊNCIAS DO MAR
WEST AFRICAN SCIENCE SERVICE CENTRE ON CLIMATE CHANGE AND ADAPTED LAND USE

Master Thesis

SAHARAN DUST TRANSPORT TOWARDS THE TROPICAL ATLANTIC OCEAN AND SOUTH AMERICA: A 3-DIMENSIONAL ANALYSIS BASED ON LIVAS AEROSOL CLIMATOLOGY

MASSITAN BENY DEMBELE

Master Research Program on Climate Change and Marine Sciences

São Vicente
2023

UNIVERSIDADE TÉCNICA DO ATLÂNTICO

INSTITUTO DE ENGENHARIAS E CIÊNCIAS DO MAR

WEST AFRICAN SCIENCE SERVICE CENTRE ON CLIMATE CHANGE AND ADAPTED LAND USE

Master Thesis

SAHARAN DUST TRANSPORT TOWARDS TROPICAL ATLANTIC OCEAN AND SOUTH AMERICA: A 3-DIMENSIONAL ANALYSIS BASED ON LIVAS AEROSOL CLIMATOLOGY

MASSITAN BENY DEMBELE

Master Research Program on Climate Change and Marine Sciences

Supervisor | Prof. Dr. Nilton Évora do Rosário

Co-supervisor | Dr Eleni Marinou

São Vicente
2023

UNIVERSIDADE TÉCNICA DO ATLÂNTICO

INSTITUTO DE ENGENHARIAS E CIÊNCIAS DO MAR

WEST AFRICAN SCIENCE SERVICE CENTRE ON CLIMATE CHANGE AND ADAPTED LAND USE

Saharan dust transport towards tropical Atlantic Ocean and South America: a 3-dimensional analysis based on Livas aerosol climatology

Massitan Beny Dembele

Master's thesis presented to obtain the master's degree in Climate Change and Marine Sciences, by the Institute of Engineering and Marine Sciences, Atlantic Technical University in the framework of the West African Science Service Centre on Climate Change and Adapted Land Use

Supervisor

Prof. Dr. Nilton Évora do Rosário

Federal University of São Paulo - Brazil

Co-supervisor

Dr. Eleni Marinou

National Observatory of Athens

São Vicente

2023

UNIVERSIDADE TÉCNICA DO ATLÂNTICO

INSTITUTO DE ENGENHARIAS E CIÊNCIAS DO MAR

WEST AFRICAN SCIENCE SERVICE CENTRE ON CLIMATE CHANGE AND ADAPTED LAND USE

Saharan dust transport towards tropical Atlantic Ocean and South America: a 3-dimensional analysis based on Livas aerosol climatology

Massitan Beny Dembele

Panel defense

President

Prof. Dr. Neusa Pinheiro

Examiner 1

Professor Dimitris Balis

Examiner 2

Dr Michael Ochei

São Vicente
2023

Financial support

The German Federal Ministry of Education and Research (BMBF) in the framework of the West African Science Service Centre on Climate Change and Adapted Land Use (WASCAL) through WASCAL Graduate Studies Programme in Climate Change and Marine Sciences at the Institute for Engineering and Marine Sciences, Atlantic Technical University, Cabo Verde.

Dedication

This work is dedicated to my dead father Beny Dembele, and Maimouna Koita, who have been unwavering in their support of me throughout my training through prayer, and everyone, who has contributed to my education.

Acknowledgments

First, I would like to thank Almighty God for his unconditional blessings, without which this would not have been a reality today.

I am greatly thankful to my supervisor Prof. Dr. Nilton Évora do Rosário for his advice and for being an inexhaustible source of motivation and inspiration. Working with him has always motivated me to work hard, to be diligent, and to do better. I really appreciate working under your directive during these six months.

Special thanks to my co-supervisor Dr. Eleni Marinou, for their encouragement and for giving me the opportunity to discover this new field.

I also express my heartfelt gratitude to Manoli, Thanasis Georgiou, and the National Observatory of Athens (NOA) for giving me the LIVAS dataset.

My deepest gratitude to the remote sensing team of TROPOS for their availability and assistance during and after my internship at TROPOS, especially to Dr. Holger Baars, Dr. Julian Hofer, Dr. Athena Augusta Floutsi, and Ina Burkert.

I would like to thank the Director of WASCAL Cabo Verde, Prof. Dr. Corrine Almeida, the Deputy Director, Dr. António Pinto Almeida, the scientific coordinator Dr. Estanislau Baptista Lima, and all the staff for all their support and constructive criticism during different stages of my studies.

I acknowledge the Ministry of Education and Research (BMBF) for founding this great program. In addition, huge thanks to Universidade Técnica do Atlântico (UTA) – Cabo Verde for hosting this program

Finally, to thank all my friends and WASCAL colleagues in Cabo Verde for their help, moral support, and late-night feedback sessions, who influenced and inspired me.

Resumo

Compreender a distribuição espacial das partículas de aerossol é essencial para a avaliação de sua influência no sistema climático. A poeira do Saara Como um componente fundamental do sistema global de aerossóis requer uma análise integrada da sua estrutura espacial. O principal objetivo desta pesquisa foi estudar a estrutura da poeira do Saara sobre a cidade de Mindelo, em Cabo Verde, e durante o seu transporte para áreas remotas do Atlântico tropical e das Américas utilizando o recentemente desenvolvido LIVAS (*LIdar climatology of Vertical Aerosol Structure for space-based lidar simulation studies*), um banco de dados óptico global 3-D de aerossóis baseado em produtos do satélite CALIPSO. A dependência dos produtos do LIVAS em relação ao raio utilizado para agregar os perfis CALIPSO também foi avaliada. Uma comparação preliminar nas escalas diária e mensal entre os perfis de retroespalhamento e coeficiente de extinção do LIVAS e do PollyXT, um sistema lidar de superfície operado em Mindelo, indicou uma boa concordância. A aplicação das propriedades ópticas colunares e verticais do LIVAS para caracterizar a variabilidade sazonal da poeira do Saara sobre o Mindelo mostrou que a maior parte do transporte ocorre de Junho a Setembro e tem seu máximo entre 2 e 5 km de altitude. Durante a temporada de inverno, de Dezembro a Janeiro, a carga de aerossóis na troposfera livre é drasticamente reduzida, e a maior parte da poeira é transportada dentro da camada limite marinha (MBL). A contribuição da poeira para o perfil de retroespalhamento durante o verão variou de ~90% na troposfera livre (de 2 a 6 km) a menos de 25% na MBL. No inverno, a contribuição na troposfera livre é reduzida para menos de 50%. No que diz respeito à dependência do raio de agregação, a principal dependência encontrada foi a de *Dust Optical Depth* (DOD) mensal, com raios menores (<200 km) produzindo valores climatológicos mais baixos quando comparados com raios maiores. A aplicação do LIVAS para descrever o transporte sazonal da poeira do Saara para áreas remotas do Atlântico tropical e das Américas indicou padrões consistentes com os estudos anteriores. O transporte de poeira, identificadas pelo perfil de extinção, é maior no verão e primavera boreal e menor no outono. O deslocamento para norte da poeira é maior durante o verão, atingindo a latitude de 25ºN. Este deslocamento é modulado pela migração sazonal da zona de convergência intertropical (ITCZ), e favorece o transporte de poeira para a América Central e o Caribe. O inverno é a estação em que chega a menor quantidade de poeira no Atlântico tropical oeste e Américas, o que pode ser explicado pelo transporte de baixo nível de poeira e uma remoção eficiente de poeira ao longo de seu caminho. Neste período o principal receptor continental da poeira é a América do Sul.

Palavras-chave: Pluma de poeira do Saara, Cabo Verde, Profundidade Óptica de Poeira, LIVAS, Coeficiente de Extinção, PollyXT.

Abstract

Understanding the spatial distribution of aerosol particles is essential to evaluating their influence on the climate system. Saharan dust plume as a fundamental component of the global aerosol system requires a comprehensive analysis of its spatial structure. The main objective of this research was to study the Saharan dust plume structure over Mindelo City, in Cabo Verde, and during its transport towards remote areas of tropical Atlantic and Americas using the recently developed LIdar climatology of Vertical Aerosol Structure for space-based lidar simulation studies (LIVAS), a 3-D multi-wavelength global aerosol optical database based on CALIPSO satellite products. LIVAS products' dependence on the radius used to aggregate CALIPSO profiles was also evaluated. A preliminary comparison of daily and monthly scales of the backscatter and extinction coefficient profiles between LIVAS and PollyXT, a ground-based lidar system operated at Mindelo City, indicated a good agreement. The application of LIVAS columnar and vertical optical properties products to characterize the seasonal variability of Saharan dust transport over Mindelo shows that most of the dust transported occurs from June to September and has a maximum of 2 to 5 km. During the winter season, from December to January, aerosol loading in the free troposphere is dramatically reduced, and most of the dust is transported within the (MBL,) in a layer up to ~2.5 km. Dust mean contribution to the backscatter profile during summer varied from ~90% in the free troposphere to less than 25% in the MBL. In the winter, the contribution in the free troposphere is reduced to less than 50%. Regarding the dependence on the aggregation radius, the main dependence found was for monthly (DOD), with smaller radii (<200 km) producing lower climatological values when compared with larger radii. The LIVAS application, which describes the seasonal transport of Saharan dust to remote western areas of the tropical Atlantic and Americas, also depicted patterns that are consistent with previous studies. The magnitudes of dust transport, as identified by the extinction coefficient profile are highest in boreal summer and spring and lowest in autumn. The northward shifts of the dust plume are further during the summer, reaching the latitude of 25^{o}N. This displacement is mainly modulated by the seasonal migration of the (ITCZ), and it leads to the transport of dust toward Central America and the Caribbean. Winter is the season that the lowest amount of dust arrives in the remote western tropical Atlantic and South America, which can be explained by the low-level transport of dust and the efficient removal of dust along its way.

Keywords: Saharan dust plume, Cabo Verde, Dust Optical Depth, LIVAS, Extinction coefficient, PollyXT.

Abbreviations and acronyms

AOD	Aerosol Optical Depth
AERONET	Aerosol Robotic Network
AEW	African Easterly Waves
AEJ	African easterly jet
AMMA	African Multidisciplinary Monsoon Analysis
CALIPSO	Cloud-Aerosol Lidar and Infrared Pathfinder Satellite Observation
CALIOP	Cloud-Aerosol Lidar with Orthogonal Polarization
CCN	cloud condensation nuclei
CVO	Cape Verde Atmospheric Observatory
DOD	Dust Optical Depth
DJF	December January February
EARLINET	European Aerosol Research Lidar Network
ENSO	El Niño-Southern Oscillation
ESA	European Space Agency
IN	ice nuclei
ITCZ	Intertropical Convergence Zone
JJA	June July August
LIDAR	Light Detection and Ranging
LIVAS	LIDAR climatology of Vertical Aerosol Structure
LRT	long-range transport
MAM	March April May
MERRA-2	Modern-Era Retrospective analysis for Research and Applications
NAO	North Atlantic Oscillation

NASA	National Aeronautics and Space Administration
NOA	National Observatory of Athens
SAL	Saharan Air Layer
SHL	Saharan heat low
SON	September October November
TROPOS	Leibniz Institute for Tropospheric Research
Tg	Teragrams
VFM	vertical feature mask
WAM	West African Monsoon
PHOTONS	PHOtométrie pour le Traitement Opérationnel de Normalisation Satellitaire

List of contents

Figure index

Table index

1. Introduction

The Sahara desert in North Africa is the world's largest dust source and contributes to over 50% of global dust emissions (Kok *et al.*, 2021). Saharan dust particles are uplifted by strong surface winds and then transported downwind for long distances, reaching the Atlantic Ocean, the Caribbean, America, and Europe (Prospero *et al.*, 1981, Ben-Ami *et al.*, 2012;). The Saharan dust emission varies daily, seasonal, annual, and even decadal time scales, largely modulated by local wind speed, land surface cover, and soil moisture (Kok *et al*., 2021; Ryder *et al*., 2018). The Saharan dust plume has large consequences for air quality in downwind settlements (Kishcha *et al.*, 2005). Given its direct influence on radiative budget due to scattering, absorption, and emission of solar and terrestrial radiation (Balkanski *et al*., 2007), as well as in cloud formation, radiative properties, and lifetime (DeMott *et al*., 2003; Koren *et al.*, 2010). Saharan dust has been regarded as a critical system to understanding the climate process within the Tropical Atlantic domain and beyond, including the American continent. However, the Saharan dust plume influence strongly depends on its spatial structure and loading, aspects highly prone to the seasonal cycle and interannual variability of atmospheric processes. Regarding its vertical distribution, for example, dust particles will have a stronger impact on shortwave radiation absorption when they are located above bright clouds (Wainker *et al*., 2013). Moreover, dust's atmospheric lifetime is much longer in the free troposphere than in the planetary boundary layer, and, upon entering the free troposphere, dust particles can be transported across vast areas, altering the geographic pattern of their impacts (Prospero & Lamb *et al*., 2003).

Additionally, mineral dust contains iron, phosphorus, and other nutrients, and could affect ocean biogeochemistry and fertilize tropical forests upon downwind deposition (Rizzolo *et al.*, 2017). Therefore, there is great interest in understanding factors controlling the Saharan dust emission, transport, and deposition towards the Tropical Atlantic Ocean and beyond, especially to the Americas, and the impact they might have on the environment, ecosystem, and climate. To this end, accurate monitoring and representation in climate models of the horizontal and vertical structure (3-D) of the Saharan dust plumes transported toward America is of great importance. However, many aspects affect Saharan plumes' 3-D structure when leaving North Africa and crossing the Tropical Atlantic.

Dust particles are removed from the atmosphere by both dry and wet deposition (Stuut *et al*., 2005; Knippertz & Stuut *et al.*, 2014). Wet deposition of dust potentially increases the

bioavailability of nutrients carried with the dust particles (Meskhidze *et al*., 2005), which can lead to an increased fertilization effect of dust deposition in the oceans (Ridame *et al.*, 2014). Dust outbreak events are usually associated with easterly waves, which emerge from the coast of Africa. These waves have a complex dynamic Structure, producing complex dust distribution patterns (Karyampudi and Carlson *et al*., 1988).

Concentrations aloft are usually several times greater than in the marine boundary layer (depending on the season), another important feature related to the 3-D structure of dust transport that has implications for its climate impacts. Seasonally, the transport structure is strongly tied to the displacement of the Inter-Tropical convergence Zone, (Moran-Zuloaga *et al*., 2018).

Due to the southernmost position of the ITCZ during the boreal winter, dust particles are then frequently transported toward the South American continent (Di *et al*., 2015). Meanwhile, the northward shift of the ITCZ during the boreal summer limits the transport to the Caribbean, Central, and North America (Prospero *et al*., 1972). In addition to the influence of seasonal oscillation of ITCZ, the export structure of North African dust towards the Atlantic and Americas also highly varies on daily and inter-annual scales. For the daily scale, the dust plume structure is largely affected by the meteorological condition (e.g. precipitation), while climate variability modes, for example, El Niño-Southern Oscillation (ENSO) and North Atlantic Oscillation (NAO), have been linked to the inter-annual variability in dust transport from North Africa (Barkley *et al*., 2022). Consequently, the evaluation of the simulation of the Saharan plume structure and its temporal multi-scale variability in the climate models can provide insights about the model performance that go beyond the plume structure. However, a comprehensive monitoring framework of Saharan dust transport is of fundamental importance.

A comprehensive understanding of the Saharan dust plume structure when transported towards the Tropical Atlantic and Americas requires a dataset that can fulfill both multi-temporal and 3-D spatial scale characterization. For a long time, 2-D climatological structure based on passive remote sensing has been the main source of information regarding Saharan dust transport toward the Atlantic, which lacked the vertical perspective. In recent decades, with the new developments in the active remote sensing of aerosols from satellites, 3-D global aerosols have emerged (Omar *et al*., 2009, Amiridis *et al.*, 2014; Marinou *et al*., 2017). These new products provide a unique opportunity to improve our knowledge of the seasonal cycle and interannual structure of dust plumes being transported from North Africa to remote regions of the Tropical Atlantic and Americas, as well as to improve our comprehension of its interaction

with other climate elements and processes (Mamouri & Ansmann, *et al*., 2016). This was the main motivation for the current research. The LIDAR climatology of Vertical Aerosol Structure for space-based LIDAR simulation studies (LIVAS) based on CALIPSO (Cloud-Aerosol Lidar and Infrared Pathfinder Satellite Observations) observations at 532 nm and 1064 nm are among the recently developed 3-D aerosol dataset (Amiridis *et al*., 2015; Marinou *et al*., 2017). As they evolve, continuous evaluation and analysis of the aerosol products of datasets such as LIVAS, under distinct atmosphere scenarios is crucial to establish their role as an observational reference, able to be used to understand the aerosol dynamics and to validate climate models (Marinou *et al*., 2017; Georgoulias *et al.*, 2018). Undoubtedly, the Saharan dust transport structure towards the Atlantic provides a unique dust aerosol scenario to evaluate LIVAS. Therefore, we selected it as the focus of the present study.

Under the question, "How does LIVAS 3-D aerosol product depict the structure and seasonality of Saharan dust transport toward tropical Atlantic and Americas?" this thesis searched to achieve the objectives subsequently described.

1.1. Objectives of the work

The aim objective of this thesis is to determine the spatial and temporal features of Saharan dust 3-D structure and transport towards Tropical Atlantic and Americas using the LIDAR climatology of Vertical Aerosol Structure for space-based LIDAR simulation studies (LIVAS) 3-D multi-wavelength global aerosol optical properties database.

We defined the following specific objectives to achieve the main goal:

- Evaluation of LIVAS 3-D aerosol profiles over Mindelo, Cabo Verde, via comparison with an independent Lidar system (PollyXT),
- Evaluate the seasonal cycle of all aerosols and dust profiles over Mindelo City,
- Characterization and description of the annual features and seasonal cycle of Saharan dust 3-D structure and transport towards Tropical Atlantic and Americas.

2. Literature review

2.1.1. The importance of Saharan dust

North dust emission and transport historically have attracted the attention of the climate scientific communities due to its importance regarding the global energy and hydrological cycles, human health, marine and continental ecosystems. Aerosol systems, such as Saharan dust, can affect climate directly by scattering and absorbing solar radiation and indirectly by modifying radiative properties (Ramanathan *et al.*, 2001), cloud microphysical effects such as cloud condensation nuclei directly and indirectly (Wurzler *et al.*, 2000) or ice nuclei (DeMott *et al.*, 2003). Moreover, the Saharan dust plume plays an important role in biogeochemical processes across the world, especially in tropical Atlantica and America. Deposits on land surfaces, therefore, contribute to soil development (Muhs *et al.*, 2007) and as a source of nutrients (e.g., Swap *et al.*, 1992). Ocean supplies of iron (Jickells *et al.*, 2005; Mahowald *et al.*, 2005), and phosphorus which are essential elements for phytoplankton growth and, hence, for the oceanic and global carbon cycle (Mahowald *et al.*, 2008). Under favorable weather conditions, a large amount of mineral dust can be injected into the free troposphere, where medium and long-range transport takes place (Ansmann *et al*., 2003), therefore, affecting remote regions.

Saharan dust is associated with dry, warm air and anticyclonic circulation. (Prospero *et al.*, 1972). Some studies suggest that North African dust may have significant effects on clouds and precipitation (Kaufman *et al.*, 2005) and possibly on the formation/intensification of tropical cyclones (Dunion & Velden *et al*., 2004; Kaufman *et al.*, 2005).

2.1.2. Saharan dust emission and transport towards tropical Atlantic: Main aspects

The processes of generating and transporting dust are complex and still matters of ongoing research since dust particles play a crucial role in geochemical and geophysical processes. To these processes, one can also include the addition of nutrients to soils and oceans. The Saharan dust transport is influenced by many factors African Easterly Jet, Saharan Air Layer, Saharan Heat Low, West African Westerly Jet, African Westerly Jet, Tropical Easterly Jet, ITCZ, Easterly waves, Azores Anticyclone, among others aspects such as multi-scale climate variability modes as ENSO (Emily Bercos *et al.*, 2020).

The meteorological conditions in the dust-source regions, which are highly variable, are the primary determinant of dust emission. Saharan dust plumes can travel over long distances in

the atmosphere via three main pathways. The first pathway is across the Atlantic Ocean to North America, the Caribbean, and South America (Prospero & Lamb *et al.*, 2003). The second pathway is towards the Mediterranean and Europe (Marinou *et al.*, 2017; Moulin *et al.*, 1998). The third pathway is towards the eastern Mediterranean and the Middle East (Israelevich *et al.*, 2003).

North African dust transported over the tropical Atlantic is one of the main long-range transport paths. Dust transport follows more southward trajectories driven by strong northeasterly winds (Harmattan), bringing dust to most parts of Nigeria, the Gulf of Guinea (Washington *et al*., 2006a), and as far as the Amazon Basin in South America (Kaufman *et al*., 2005). In short, In-situ observations of African dust in Barbados date back to 1965. This provides a long-term climatology of the route over the northern tropical Atlantic. (Prospero & Carlson *et al*., 1980). During boreal summer, the preferred pathway is to the Caribbean, with dust transported within an atmospheric layer up to 5–6 km height.

A mass of dusty air known as the Saharan Air Layer (SAL) forms over the Sahara Desert during the late spring, summer, and early fall. The SAL moves westward across the tropical North Atlantic covering the Island of Cabo Verde, which has been used as a reference site to characterize Saharan dust plume properties at the beginning of its journey down the tropical Atlantic. During hurricane season, the SAL plays an important role. Large amounts of dust create a stable layer of dry, sinking air that can suppress hurricane development (Zipser *et al*., 2009).

The dust emission and transport from North Africa are known to exhibit variability on diurnal to decadal timescales. Concerning the annual cycle, in the dry season or winter dust transport from the Sahara and Sahel follows a more southwards trajectory towards the Gulf of Guinea. Surface wind speeds follow a clear annual cycle, with a maximum during the winter months and a minimum between July and September. During the dry season, the dust layer is transported in a southwest direction and is situated within the lowest 2 km of the troposphere and frequently transported to Cabo Verde (Chiapello & Moulin *et al.*, 2002; Schepanski *et al.*, 2009).

The inter-annual variability of dust emission of transport from North Africa is discussed in connection with the controlling atmospheric dynamics (Evan & Mukhopadhyay *et al*., 2010). The positioning and intensity of the ITCZ have been linked to this phenomenon (Doherty *et al*., 2014). A low-pressure zone located around the equator where the northeast and southeast

trade winds converge constrains precipitation and long-range dust transport to important regions such as the Amazon basin. Due to higher solar radiation levels near the equator, The ITCZ forces the air to rise to the upper troposphere. It then moves towards higher latitudes and slowly descends, leading to large high-pressure areas in the subtropics. The latitudinal position of the ITCZ varies seasonally following the insolation annual cycle.

The intra-seasonal variability of North African dust emissions within a season range on time scales of several days. Dust outbreaks over the Atlantic are associated with warm phases of the Saharan heat low (SHL). These warm phases favor the emission from dust sources in the western Sahara and simultaneously intensify the mid-tropospheric African easterly jet (AEJ), opening the route to the west (Wang *et al.*, 2017). A synoptic-scale feature of the North African circulation system known as African Easterly Waves (AEW) may play an important role in dust mobilization during the boreal summer (Jones *et al*., 2003, 2004).

2.1.3. Dust remote sensing

Satellite-based remote sensing of the atmosphere has become one of the most important techniques for the observation of the global atmospheric composition over the last few decades. Satellites provide opportunities to observe the entire Earth. Historically, satellite-monitoring systems based on passive remote sensing shaped the vertical structuration of dust plume transport. The Lidar technique has proven to be a very useful tool in atmospheric profiling research since it provides information on several atmospheric parameters with high vertical spatial and temporal resolution.

The vertical structure of the Saharan dust transport westward is usually described using height-latitude cross-sections of the westward dust transport across different meridians. Most of our knowledge on the vertical structure of dust plumes results from aircraft and surface-based and satellite-borne aerosol Lidar systems. While the former two are usually restricted to field campaigns or locations relatively far away from Saharan dust sources, space-borne CALIPSO now provides north-south cross-sections through Saharan dust plumes in cloud-free regions and three-dimensional structures, transport patterns across the Atlantic Ocean, and their accompanying meteorological properties. Lidar measurements are an appropriate tool to study the optical properties of dust as only they allow one to identify suspended Saharan dust layers even in cases when different aerosol types are present in the atmospheric column. One of the key parameters for characterizing an aerosol type is the LIDAR ratio (i.e. the ratio between

extinction and backscatter coefficients), which can be determined with Raman LIDAR. (Ansmann *et al*., 1990).

The Lidar ratio is required as input data for the quantitative determination of particle extinction profiles in the case of standard ground and space backscatter LIDAR (e.g. CALIPSO (Winker *et al.*, 2007). Extinction is one of the key parameters for calculating radiation fluxes. Determining the particle depolarization ratio from depolarization Lidars also requires the use of the LIDAR ratio. (Biele *et al*., 2000). EARLINET (Pappalardo *et al*., 2014), operates advanced LIDAR systems employing depolarization techniques that have been invaluable for dust research. Moreover, the sophisticated methodologies developed in EARLINET make it possible to characterize all types of aerosols, including dust. (Papayannis *et al.*, 2008) although the contribution of dust to the total aerosol load (Tesche *et al*., 2009).

2.2. Saharan dust seasonality

Gläser *et al.*, (2015) results confirmed the previously observed preferential trajectories of transatlantic dust. During boreal winter and spring, African dust is mainly transported below 800 hPa toward South America. Mauritania and Mali are the locations where the Saharan dust main source is found in JJA. Bodélé Depression located in the southern edge of the Sahara Desert in north-central Africa, is a major source of atmospheric dust and it's becomes the main area source in DJF when the dust is mainly transported to and deposited to the south and southwest. Over the Atlantic, most of the dust is transported toward South America in DJF and MAM, and the zonal transport to the Caribbean is prevalent in JJA and SON.

Marinou *et al*., (2017), studied dust transport from North Africa to Europe and found that during spring the spatial distribution of dust shows a uniform pattern over the Sahara desert, while during summer, the dust activity is mostly shifted to the western part of the desert. Throughout the year, elevated dust plumes extending up to latitudes of 40°N were observed at various heights between 2 and 6 km. The study was based on a dataset of CALIPSO dust aerosol profiles over 9 years (2007-2015), and the results reveal for the first time the evolution of dust in 3D and the seasonal patterns of dust on its transport routes from the Sahara to the Mediterranean and continental Europe.

Schepanski *et al*.,(2012), results showed that the Bodele dust's maximum contribution to Cape Verde islands' occurs in winter when this source area is the most active and dominant with regard to activation frequency and dust emission. Saharan dust transport differs significantly between summer and winter. During the winter season, near-surface layers over tropical

latitudes above trade winds inversion have maximum dust concentration with maximum westward transport at lower subtropical latitudes. The vertical distribution of dust zonally exported clearly shows that meridional dust export is related to general circulation patterns that are mainly controlled by Hadley circulation.

3. Materials and Methods

3.1. Study area

The study area covers a domain that extends from North Africa to the northern portion of South America, including most of the Tropical Atlantic (Figure 1). North Africa is the biggest source of dust in the world due to favorable climatic and geological conditions. With its enormous extension, it emits about 800 Teragrams (Tg) of dust into the atmosphere annually, which represents 70% of the global emission of this type of particle. (Huneeus *et al.*, 2011; Prospero & Mayol-Bracero *et al.*, 2013).

Atmospheric dynamics over the region favor strong emission, as well as transport of dust to the tropical Atlantic, making North Africa the largest exporter of dust to the tropical Atlantic and the Americas. As the tropical Atlantic has a significant influence on global climate, scientific data on this region is very important. Cabo Verde lies directly in the path of the sandstorms that migrated westwards from the North African region to the Atlantic Ocean. Therefore, the local population is exposed to serious health and other risks related to the dust plumes. There is a need to strengthen atmospheric dust monitoring capacities in the region for both climate and air quality studies. On the other hand, remote continental ecosystems such as the Amazon rainforest in South America rely on Saharan dust transport to get their needed nutrients. The continental regions of the Americas affected by transport vary according to season (Figure 1). During boreal summer, transport mainly affects the southern portion of North America and the Caribbean, and during boreal winter, the northern region of South America becomes the main continental receptor of Saharan dust (Joseph M. Prospero *et al*., 2014).

On their way to remote regions of tropical Atlantic and America, Sahara dust affects Cape Verde Islands and other West Africa countries all year round, depending on their location and wind regime. For this reason, Cabo Verde is a reference site to study the dust transport structure just as it starts its displacement over the Tropical Atlantic.

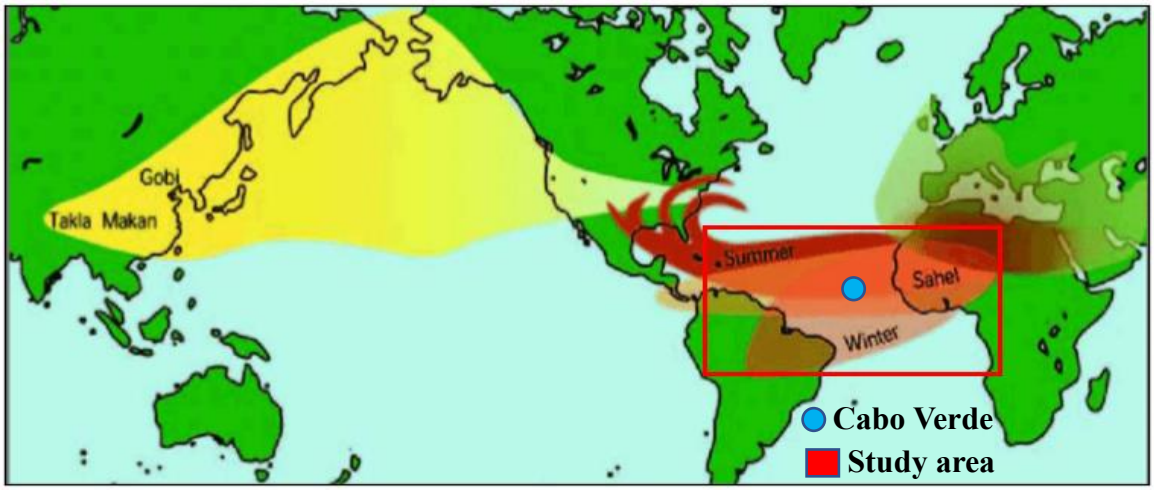

Figure 1: The two major global dust transport systems in the world: (1) from the Sahara and Sahel of Africa to the Americas and Europe; and (2) from the Takla Makan and Gobi deserts of China, across China, Korea, Japan, and the northern Pacific to North America.The study area of the present study (red box) covers from North Africa to the northern region of South America and the Tropical Atlantic. Illustration: Betsy Boynton. (Garrison *et al*., 2003).

The influence of dust on the environment varies from region to region within the study area, causing problems related to air quality in areas close to the source of dust emissions and for ecosystem fertilization in remote areas. For instance, Saharan dust is very important as a source of nutrients for the Amazon rainforest ecosystem, namely iron, and phosphorus. *(*Prospero *et al*., 1996, Mahowald *et al*., 2005;). When it is suspended in the atmosphere, one of the main climatic effects of Saharan dust particles is related to their potential or ability to alter the balance of radiative energy in the atmosphere and at the surface by scattering, absorbing solar, and terrestrial radiation (Kaufman *et al*., 2002). Consequently, studies in the region aimed at advancing current knowledge of the optical properties of mineral dust and its effects on climate are extremely important.

3.2. Data Analysis

3.2.1. LIVAS Aerosol Product

The LIVAS is a 3-dimensional aerosol and cloud product sponsored by the European Space Agency (ESA) that provides information on the vertical structure of aerosol optical properties on a global scale (Amiridis *et al*., 2015). It is based on CALIPSO (Cloud-Aerosol Lidar and Infrared Pathfinder Satellite Observations) Level 2 (L2) products, which include aerosol and cloud backscatter and extinction coefficients at 532 nm and 1064 nm as well as the linear

particle depolarization ratio at 532 nm) (Marinou *et al*., 2017). The CALIPSO mission is a collaboration between NASA and Centre National d'Études Spatiales and was launched together with the Cloud Sat satellite in April 2006. It is now flying in formation with the A-train constellation of satellites (Stephens *et al*. 2002). CALIPSO is a LIDAR instrument that is designed to acquire vertical profiles of the backscattered signal at 532 nm and a total backscattered laser signal at 1064 nm from a near nadir-viewing geometry. To produce the extinction profiles included in the Level 2 products, the CALIPSO algorithm separates free-cloud atmospheric aerosol layers according to the aerosol subtype (i.e., dust, polluted dust, clean continental, polluted continental, marine, and smoke) using information on surface type, layer integrated attenuated backscatter, the depolarization ratio at 532 nm and aerosol height (Marinou *et al*., 2017). The aerosol extinction profile is retrieved by assigning the lidar ratio for each atmospheric altitude based on the inferred subtype at each layer. In the LIVAS aerosol products, pure dust extinction is also available based on (Amiridis *et al*., 2013) methodology. To obtain pure dust extinction profiles, (Amiridis *et al*., 2013) method decoupled the dust backscatter coefficient from the total aerosol backscatter based on depolarization measurement by assuming a typical particle depolarization ratio value for pure dust equal to 0.31 (Tesche *et al.*, 2009). This value has been evaluated as a good representative of dust depolarization ratio around the world and the variation observed in Saharan dust depolarization ratio 0.25 to 0.35, (Ansmann *et al.*, 2011), is expected to introduce negligible error in the pure dust backscattering retrieval (Marinou *et al*., 2017).

Additionally, for LIVAS product, CALIPSO particle linear depolarization ratio profile is recalculated to fix known bugs (Amiridis *et al*., 2013). To ensure LIVAS product accuracy, a set of criteria originally from CALIPSO and new ones adopted are defined to identify the high-quality aerosol scene, starting by ensuring that all cloud features are removed. Further details on this can be found in (Marinou *et al*., 2017). From pure dust backscattering, the pure dust extinction coefficient is computed by utilizing a lidar ratio of 55 sr, shown to be representative of Saharan dust in distinct scenarios (over Europe, near the source, and during long-range transport (Marinou *et al*., 2017). This value is different from that used by CALIPSO in its conventional product, which is 40 sr (Omar *et al*., 2009). Finally, the spatial average of all aerosol type and pure dust backscattering and extinction coefficient profiles as well as particle linear depolarization ratio are aggregated to gridded product at 1° × 1° horizontal spatial resolution and vertical resolution of 60 m from m -0.5 to 20.2 km and 180 m from 20.2 to 30.1 km. Height is referenced to above sea level (a.s.l.) altitudes. While the LIVAS conventional

horizontal resolution was used to study long-range transport between North Africa and South America, specifically for the LIVAS product evaluation over Mindelo city, in Cabo Verve, in this study different aggregations based on the different radii (100 km, 200 km, 300 km, 400 km, and 500 km) taking Mindelo as the center were tested (Fig, 2). In order to produce Dust aerosol Optical Depth (DOD), pure dust profiles are averaged for each grid, while all non-dust aerosol extinction is assigned a value of 0 km^{-1}. The LIVAS Aerosol Optical Depth (AOD) products have been validated against AERONET presenting consistent results (Amiridis *et al*., 2013).

The National Observatory of Athens (NOA) provided the LIVAS dataset used in this study, covering a period of 16 years from January 2006 to December 2021(daily). Besides its relevance to the observational study of aerosol spatial and temporal variability and climate effects, LIVAS aerosol climatology is a very useful dataset for studies integrating other satellite products and for the evaluation of climate model performance (Georgoulias *et al.*, 2018).

$$\beta_d = \beta_t \frac{(\delta_p - \delta_{p,nd})(1 + \delta_{p,d})}{(\delta_{p,d} - \delta_{p,nd})(1 + \delta_p)} \qquad \text{(Eq: 1)}$$

Where:

β_d= is the Backscatter dust

β_t= is the Backscatter total

$\delta_{p,d}$= is Dust particle linear depolarization ratio

δ_{nd}= is the linear depolarization of Non_dust

3.2.2. PollyXT LIDAR

The Leibniz Institute for Tropospheric Research (TROPOS) has been operating a PollyXT Lidar system in Mindelo city, in the context of the Raman and polarization lidar network PollyNET, profiling a set of aerosol optical properties namely backscattering and extinction coefficients and volume depolarization ratio in the city atmosphere column (Baars *et al*., 2016).

PollyNET has been continuously improved with gained experience from EARLINET, worldwide field campaigns, and institute collaborations within the last 10 years. PollyNET lidar systems are relatively robust, as they can function unsupervised and autonomously 24 hours a day, seven days a week (24/7) (Wandinger *et al.*, 2012). One more advantage of

PollyXT Lidar is its consistent data structure and centralized data processing in line with the CIMEL Sun photometer of AERONET (Baars *et al.*, 2016)

From PollyXT an inversion algorithm, for instance, to deduce the lidar ratio, Ångström exponents, size distribution, and particle concentration, can derive backscatter and extinction coefficients and volume depolarization ratio additional information about aerosols' optical and microphysical properties. Additionally, a polarization-sensitive channel has been set up to determine the particle shape from a linear depolarization ratio, to distinguish dust and non-dust particles in mixed aerosol layers (Baars *et al*., 2011).

PollyXT backscattering and extinction coefficient profiles are provided at the same wavelength of LIVAS reference channel 532 nm. Inter-comparison between PollyXT and LIVAS profiles over Mindelo is an excellent opportunity to evaluate the agreement between the two datasets and to test PollyXT Lidar spatial representatives as the aggregation radius for the LIVAS product is gradually increased from 100 km to 500 km. The PollyXT dataset collected for September of 2021, during the ASKOS campaign in Cabo Verde, was made available by TROPOS for this task.

3.2.3. AERONET dataset

The AERONET (AErosol RObotic NETwork) program is a federation of ground-based remote sensing aerosol networks (Holben *et al*., 1998) established by NASA and PHOTONS (PHOtométrie pour le Traitement Opérationnel de Normalisation Satellitaire; Univ. of Lille 1, CNES, and CNRS-INSU). Based on CIMEL sun-photometers. It provides a worldwide long-term, continuous database of aerosol optical, microphysical, and radiative properties for aerosol research and characterization, validation of satellite retrievals, and synergism with other databases. In Cabo Verde, there are two operational sun photometers from AERONET, one in Sal Island (1994-2023) and another in Mindelo City (2021-2023) (Figure 2). In the past, AERONET sun photometers were operated on Santiago Island in (2008), and Praia City (2015), and in the eastern portion of São Vicente Island (2012-2017) at the Cape Verde Atmospheric Observatory (CVO). The network imposes standardization of instruments, calibration, processing, and distribution, which is crucial to the application of its aerosol products as a reference. AERONET sun photometers measure direct solar radiation at a 15-minute resolution and sky radiation at a 1-hour resolution. The instrument takes direct solar radiation measurements at eight different channels of 340, 380, 440, 500, 675, 870, 940, and 1020 nm (Holben *et al*., 1998). From this direct solar radiation and based on the Beer-Lambert-

Bouguer law, which describes the attenuation of spectral direct solar radiation through the Earth's atmosphere, the AERONET algorithm retrieves spectral AOD (Aerosol Optical Depth), except for the channel 940 nm, which is dedicated for measuring columnar water vapor. The uncertainty in the AOD retrieval under cloud-screen conditions for the wavelengths above 440 nm is < ± 0.01 and for shorter wavelengths < ± 0.02 (Eck *et al*., 1991). AERONET data are provided at three quality levels: level 1.0 for raw data, level 1.5 for cloud-filtered observations, and level 2.0 for quality-assured data to which post-field calibration has been carried out. Unless when it is unavailable, level 2.0 is the one considered in validation studies. The AOD at the channel 500 nm was used in this study to evaluate LIVAS AOD climatology over Mindelo City calculated by the integration of its extinction profile. AOD at 500 nm from the AERONET sun photometer at Sal Island was also used in this work as a complement to understand LIVAS spatial representativity as different radii are considered. The AERONET dataset used in this study was obtained from its official site [1] (http://aeronet.gsfc.nasa.gov/).

3.2.4. MERRA-reanalysis

Aerosol Optical depth at 550 nm from NASA reanalysis system the Modern-Era Retrospective analysis for Research and Applications, Version 2 (MERRA-2, (Randles *et al*., 2017) at hourly time scale was used to characterize aerosol horizontal distribution for the study cases of comparison between PollyXT and LIVAS over Mindelo City.

3.3. Methods

3.3.1. Aerosol profile over Mindelo city from LIVAS.

3.3.1.1 Intercomparison between Pollyxt and LIVAS

This comparison process goal was to evaluate the agreement between Pollyxt and LIVAS to reproduce monthly variability of dust (mineral dust of North Africa) data and to describe the level of agreement between them across Mindelo. Representation of Frequency per domain as a function of CALIPSO radius over Cape Verde (study domain) presented in Fig. 2. It is evident that the 100 km radius corresponds to the Mindelo site, while the 500 km radius covers the entire Cabo Verde region.

[1] http://aeronet.gsfc.nasa.gov/

3.3.2. Aerosol climatology over Mindelo based on LIVAS.

Using LIVAS products at different aggregation radii specifically developed for Mindelo City was performed, as seasonal analysis of optical depth and backscattering of extinction coefficient profiles for all aerosols and pure dust over Mindelo. Based on the traditional grouping of months considering the boreal and austral summer and winter seasons: from December to February (DJF), from March to May (MAM), from June to August (JJA), and from September to November (SON) to investigate the transport of Saharan dust to tropical Atlantic and South America.

3.3.3. Saharan dust transport

Dust aerosols significantly influence the global radiative budget by scattering and absorbing longwave and shortwave radiation. This affects the vertical profile of temperature, atmospheric stability, and precipitation. Therefore, knowledge of the vertical distribution of dust is important, the analysis will be focused on the climatological seasonality and will be analyzed using different cross-sections extending from North Africa to South America: one following the core of horizontal distribution and vertical of the two others at each side of the core. Trends and patterns that vary in the dust structure were assessed via the second specific objective, which will target inter-annual variability. We will obtain seasonal anomaly (deviation from the seasonal climatology) and use it as a reference to evaluate the transport behavior across the different years.

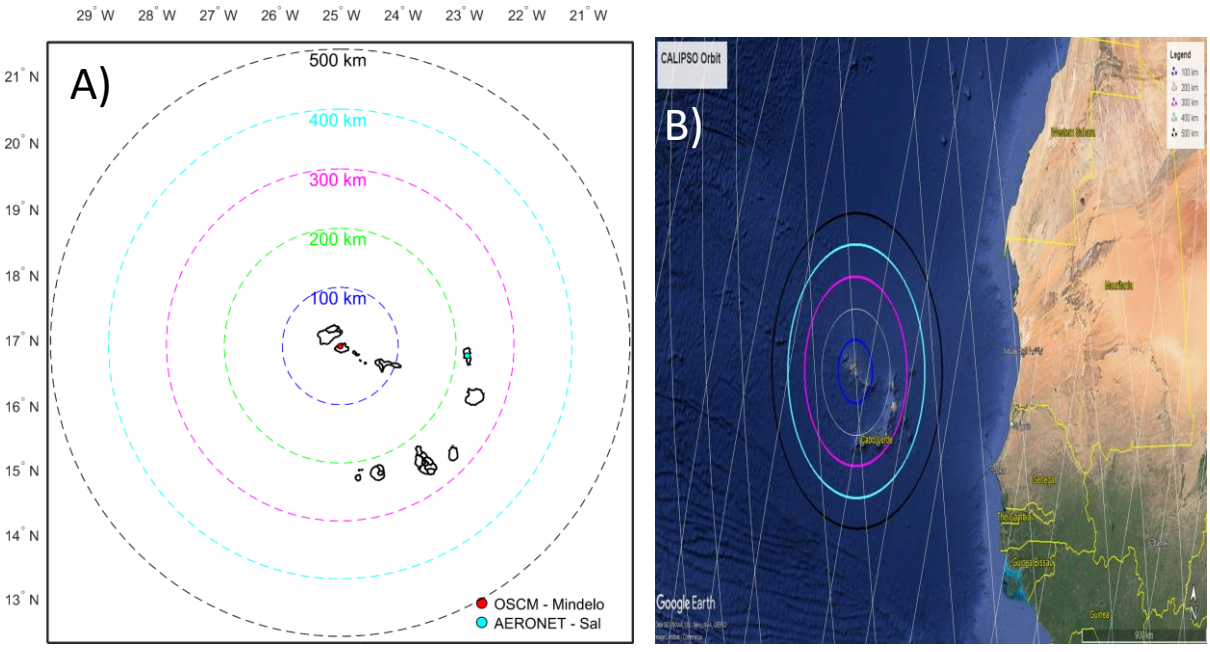

Figure 2: Distribution of the different radius and orbit (B) derived by CALIPSO over Cape Verde.

Statistical analysis is a widely used method in climatology that involves calculating the mean, median, anomalies, etc. Applied for both specific objectives, to characterize the seasonal climatology of the 3-D structure of Saharan dust and its inter-annual variability. We will use Matlab software to perform the above statistical analyses and graphical studies.

4. Results

The results of the present study are divided into 3 sections. In the first one, LIVAS and PollyXT lidar system backscattering and extinction profiles over Mindelo city are compared for September 2021 in Fig, 3-8, when the ASKOS campaign (Marinou *et al*., 2023) took place. The influence of the LIVAS aggregation radius is also evaluated. In the second section, the LIVAS long-term dataset (2006-2021) is applied to characterize the climatology of all aerosol and pure dust optical depths, backscatter, and extinction coefficient profiles over Mindelo. Finally, LIVAS long-term 3-D product is used to characterize the seasonal dust transport towards tropical Atlantic and Americas. In this last section, climatological vertical structures of dust reaching the tropical Atlantic and South America are analyzed during the transport of the Saharan dust plume.

4.1. Comparison between LIVAS and POLLY over Mindelo

This section compares LIVAS, considering different aggregation radii, and PollyXT aerosol vertical profile over Mindelo during September 2021. The analysis and results are based on the backscatter and extinction coefficients at 532 nm. Table 1 presents the list of days in September of 2021 with collocated aerosol profiles from PollyXT and from LIVAS products. For both products, availability is directly related to the presence of cloud-free conditions and certain quality assurance criteria. Specifically for LIVAS, CALIPSO distance from Mindelo is also an aspect that controls availability. As CALIPSO overpassing distance from Mindelo increases, profile availability shifts to the larger radii. The radius 500 km, consequently, is expected to enclose the highest number of profiles.

From the list presented in Table 1, only for 4 days (5, 9, 18, 22, and 26 of September), there is data for all aggregation radii. From this, two study cases were selected to illustrate and discuss the vertical structures of aerosol over Mindelo as seen by PollyXT and LIVAS considering distinct radii: September 5th and 22nd, 2021.

Table 1: List of days in September 2021 with collocated profiles between LIVAS and PollyXT detailing CALIPSO distance from Mindelo, LIVAS number of profiles QA and total, and Pollyxt number of cloud-free profiles. The availability of LIVAS profiles as a function of aggregation radii is also displayed.

Year	Month	Day	Calipso distance from Mindelo (km)	Livas-Number of profiles QA	Livas-Number of profiles Total	Polly-Number of cloud-free profiles	100 km	200 km	300 km	400 km	500 km
2021	9	5	5	167	196	7	X	X	x	x	X
2021	9	6	331	85	147	1				X	x
2021	9	8	369	83	132	3				x	X
2021	9	9	44	182	195	8	X	X	x	x	x
2021	9	10	235	97	173	10			x	x	X
2021	9	12	419	53	106	4					X
2021	9	13	140	72	188	10		X	x	x	x
2021	9	14	186	39	182	12		X			
2021	9	15	465	19	72	2					X
2021	9	17	185	96	182	9		X	x	x	x
2021	9	18	90	70	192	11	X	X	x	x	X
2021	9	21	285	96	161	20			x	x	x
2021	9	22	42	160	195	11	X	X	x	x	X
2021	9	23	320	122	150	4				x	x
2021	9	25	333	138	147	12		X		x	X
2021	9	26	54	167	194	10	X		x	X	x
2021	9	27	272	124	164	9		X	x	x	X
2021	9	29	428	80	101	5					x
2021	9	30	102	43	192	4			x	x	x

4.1.1. The first case: September 5th, 2021

Figure 3 presents the spatial distribution of AOD at 550 nm from Merra-2 reanalysis for September 5th for the closest time to CALIPSO overpassing. The aim is to show the spatial structure of aerosols across the distinct radius during this day. Therefore, the graph illustrates the 5 radii centered at Mindelo considered to aggregate LIVAS aerosol optical properties profiles. The PollyXT location in Mindelo at OCSM and AERONET sun photometer installation at Sal Island. The AOD field exhibits structures that indicate Saharan dust being

transported toward the Atlantic. Among the radius, the highest loading of aerosols are found within the 500 km radius, while less aerosol is present as one moves from 400 km to 100 km radius. Therefore, this structure indicates a highly non-uniform distribution of Saharan dust over the study domain, with most of the dust traveling northward of Cabo Verde.

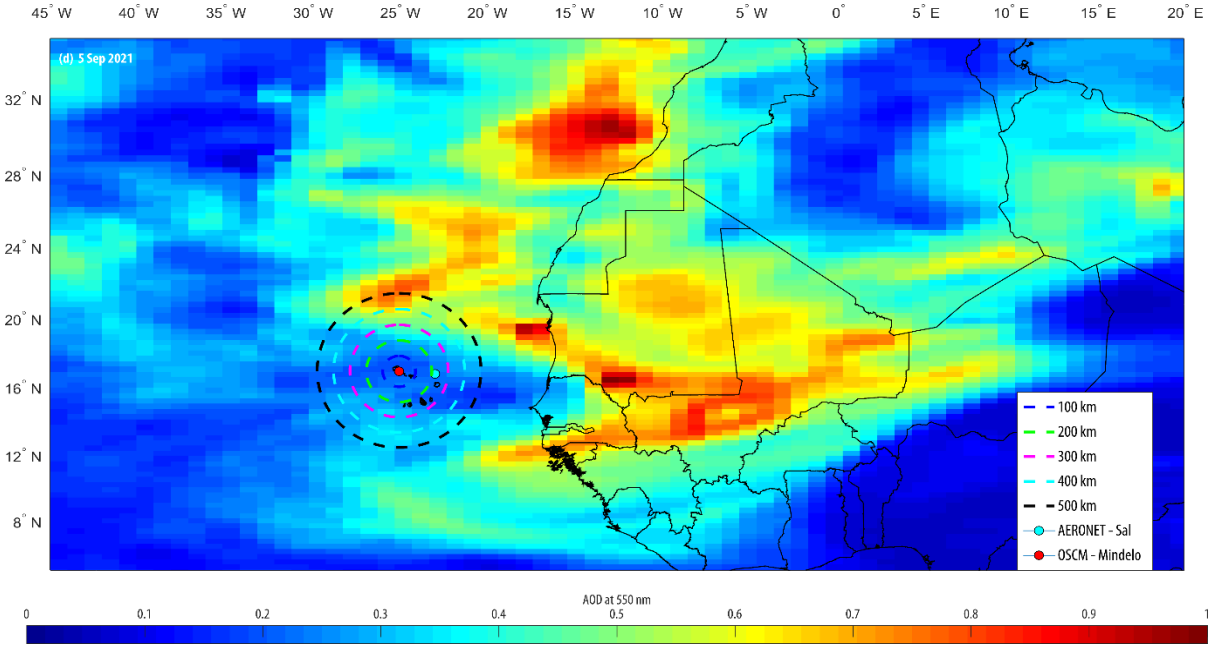

Figure 3: Spatial distribution of horizontal dust transport of AOD at 550 nm towards Cape Verde using Merra reanalysis data, LIVAS, Pollyxt, and Sal AERONET on 5 September 2021.

Figure 4 compares LIVAS and PollyXT backscatter and extinction coefficient profiles for selected radii (100, 300, and 500 km) and PollyXT particle depolarization ratio. On that day, LIVAS presented an AOD_{550nm} around 0.58 for all radii, consistent with AERONET sun-photometer retrievals, which registered a daily mean AOD 500 nm of 0.59. In general, a good agreement between PollyXT and LIVAS profiles for this day for all radii. The LIVAS backscattering profile reveals an increase from 0.002 km^{-1} sr^{-1} up to 0.004 km^{-1} sr^{-1} between the layer from 1.0 to 5.0 km, indicating a presence of an aerosols layer travelling above Cabo Verde, with its core centered between 4 and 5 km. The LIVAS and PollyXT profiles also indicate a substantial increase in the extinction coefficient up 0.15 km^{-1} between 4 and 5 km. This increase is similar for all radii. The particle depolarization ratio from PollyXT varied in this layer between 0.25 and 0.30, which is consistent with dust-type aerosols (Baars et al., 2016; Marinou et al., 2017). In addition, a lower agreement between LIVAS and PollyXT mean profiles is seen between 4.0 and 5.0 km for all radii. However, the lowest agreement at the mentioned layer occurred for the smaller radius of 100 km. A similar feature is clearer seen for the layer between 1 and 2 km, with a greater agreement for the larger radii. At lower levels (<

1 km), there is a peak up to 0.006 km^{-1} sr^{-1} at 0.5 km in Livas mean profile, and then a sharp decrease to 0.002 km^{-1} sr^{-1} for the lower height. For a particular layer, the one around 0.5 km presented the larger variability (for each specific radius) and the larger variation between the radii. From 100 km to 500 km backscattering coefficients increased from 0.006 km^{-1} sr^{-1} to values above 0.008 km^{-1} sr^{-1} and the extinction coefficient from 0.15 km^{-1} to values above 0.20 km^{-1}. The larger variability in backscattering extinction coefficients for lower levels between the radii and the smaller variability for the layer in higher levels (in LIVAS and Polly) suggest that some of this Saharan plume advancing over Cabo Verde region on September 5th was travelling close to lower levels (Figure 3). Below 0.8 km Polly backscattering and extinction profiles are affected by the overlap issue (Baars et al., 2016), therefore no information is given below 0.8 km for Polly.

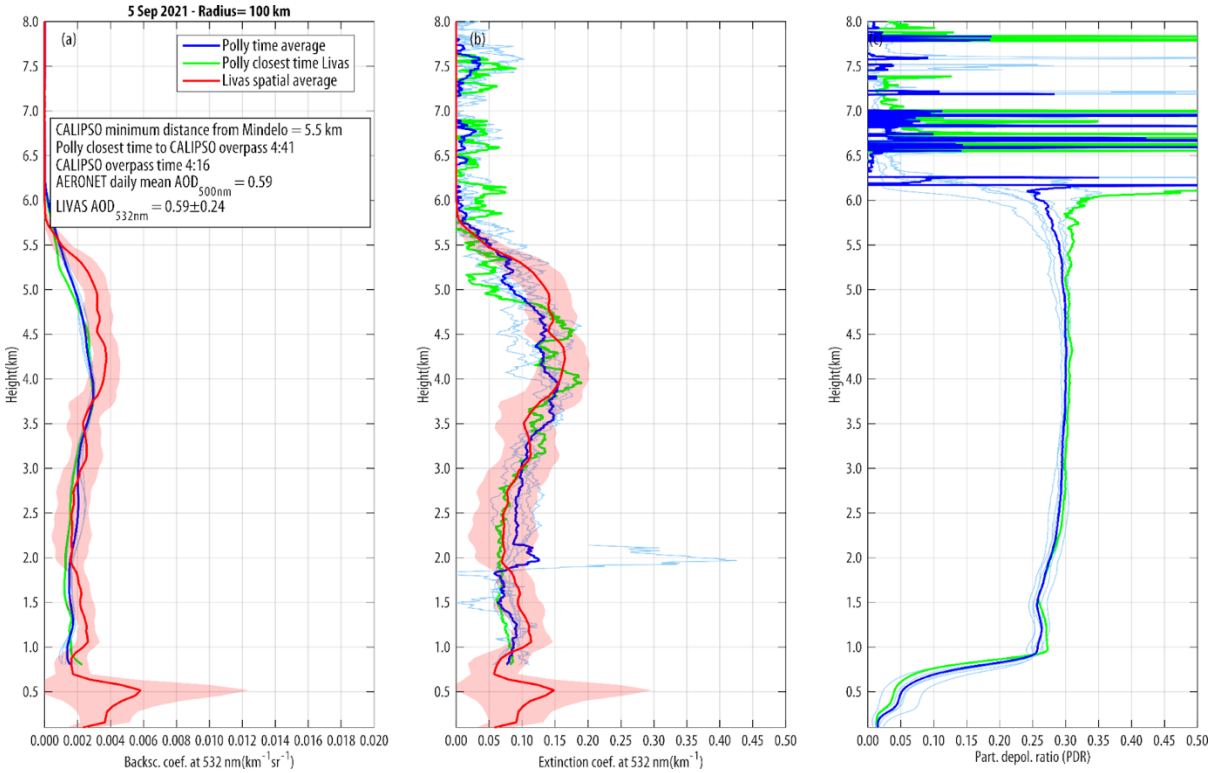

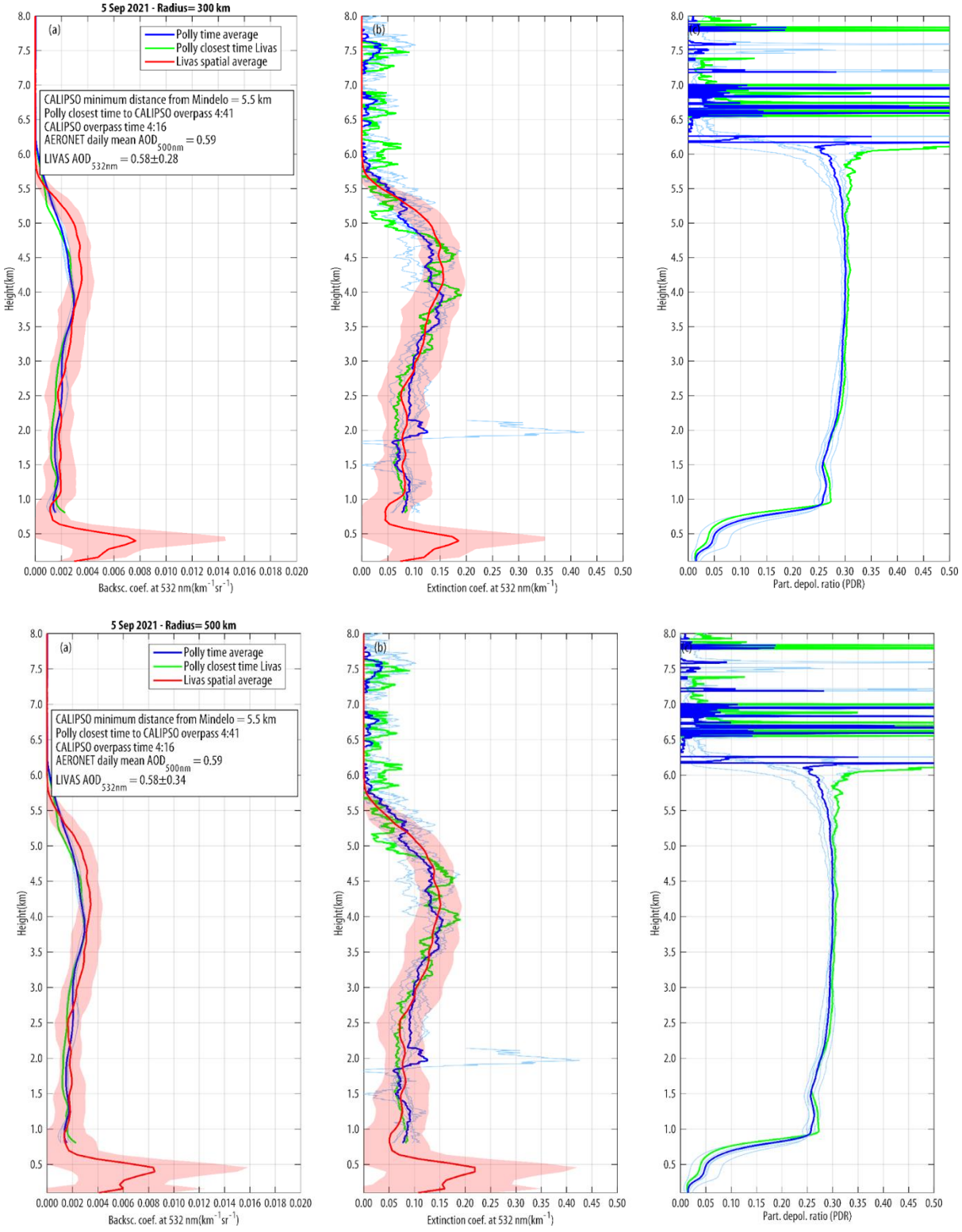

Figure 4: Comparison between LIVAS and PollyXT mean aerosol optical properties profiles for the 5 September 2021 over Mindelo city: (a) backscatter coefficients, (b) extinction coefficient. Polly particle depolarization ratio is also presented. LIVAS profiles are obtained for different aggregation radii (100, 300, and 500 km) centered at Mindelo city.

4.1.2. The second case: 22 September 2021

Figure 5 illustrates the spatial distribution of AOD at 550 nm over Cabo Verde close to the CALIPSO overpassing according to the Merra-2 on September 22nd, 2021. Cabo Verde was also under the influence of a Saharan dust plume; the eastern half of the country was under a strong influence of the plume while the second western half was experiencing lower levels of aerosol loading. On September 19, the Cumbre Vieja volcano in Las Palma started an eruption that spread large plumes of ash into the atmosphere over North Africa Atlantic coast, which certainly contributed to the regional aerosol mixture (Idrissa, 2022). From east to west of the country, AOD at 550 varied between 0.5 and 0.3. AERONET daily mean at 500 nm was 0.55 and the LIVAS spatial average varied from 0.42 to 0.44 among the radii. Different from the previous case study, CALIPSO overpassing time was not so close to PollyXT closest time to the satellite overpassing, a difference of 4 hours was identified.

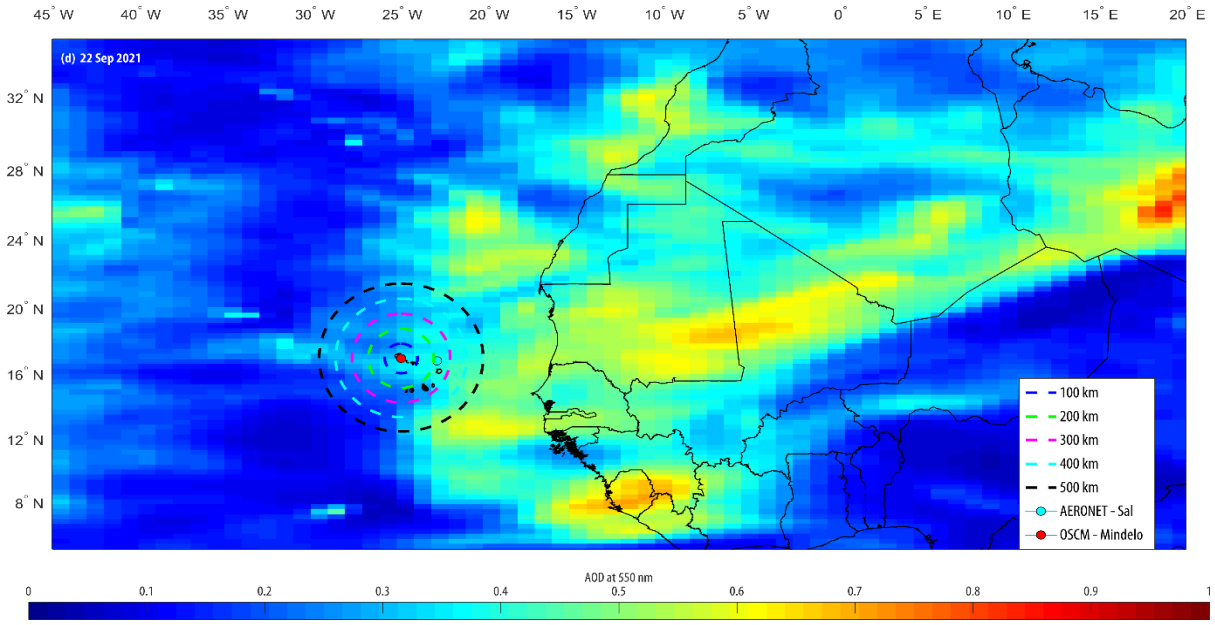

Figure 5: Spatial distribution of horizontal dust transport of AOD at 550 nm towards Cape Verde using Merra reanalysis data, LIVAS, Pollyxt, and Sal AERONET on 22 September 2021.

Figure 6, presents the comparison between LIVAS and PollyXT profiles. The extinction and backscatter profiles reveal a more stratified atmosphere in terms of aerosol layers. Two-aerosol maximum loading can be defined based on LIVAS, one centered at 2.5 km, which is dominated by dust aerosol type, as indicated by PollyXT particle depolarization ratio, and another centered at 0.6 km, which can be a mixture of marine and some dust. There are some mismatches, but a good agreement between LIVAS profiles and PollyXT profiles can be evaluated, but still not high as of September 5th. For all radii, LIVAS consistently registered a lower extinction

coefficient throughout the free troposphere when compared to PollyXT, even when considering the Polly profile that is the closest in time to CALIPSO overpassing. At lower levels (< 1. km), a higher aerosol loading was present on that day, twice that observed on September 5th, but opposite to the September 5th extinction coefficient at lower-level aerosol maximum decreased as the aggregation radii increased. On that day, PollyXT identified a higher variability in backscattering and extinction coefficients in upper levels (2.0 to 5.0 km). The Polly backscattering profile showed a variation up to 0.004 km^{-1} sr^{-1} between 3.0 and 3.5 km. For the same layer, the extinction coefficient of PollyXT up to 0.2 km^{-1}

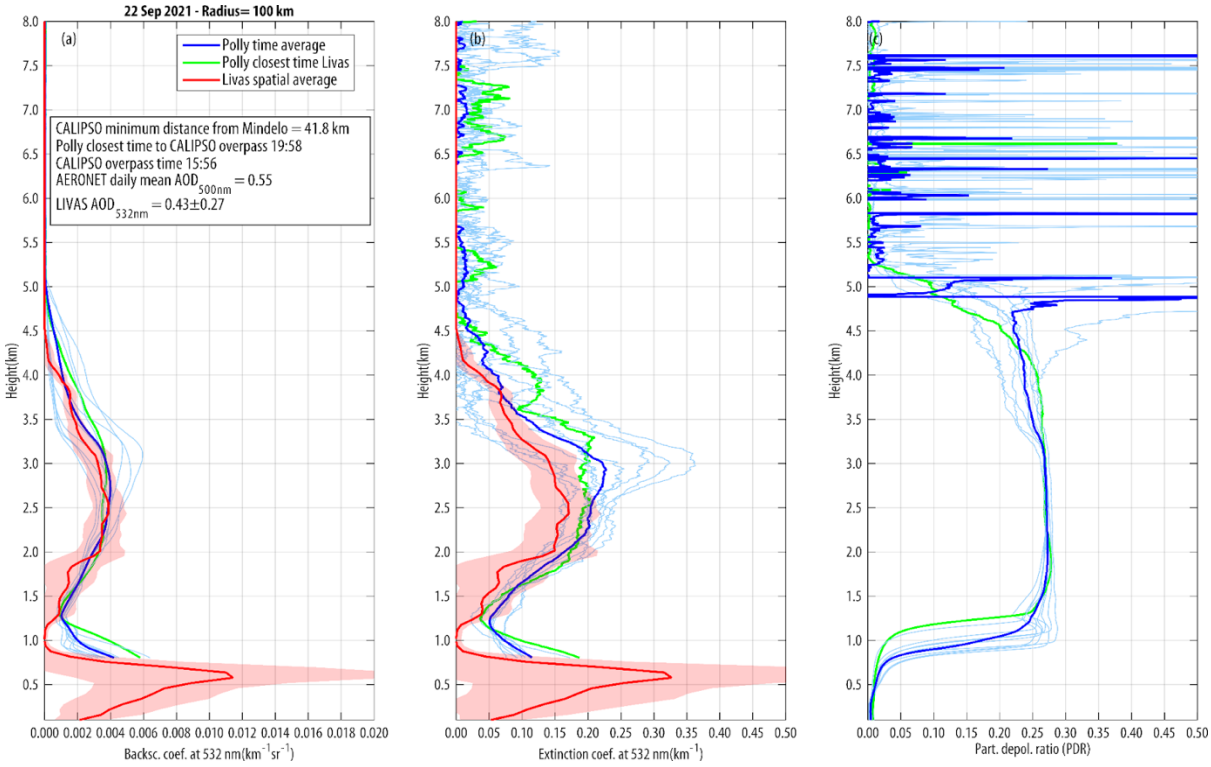

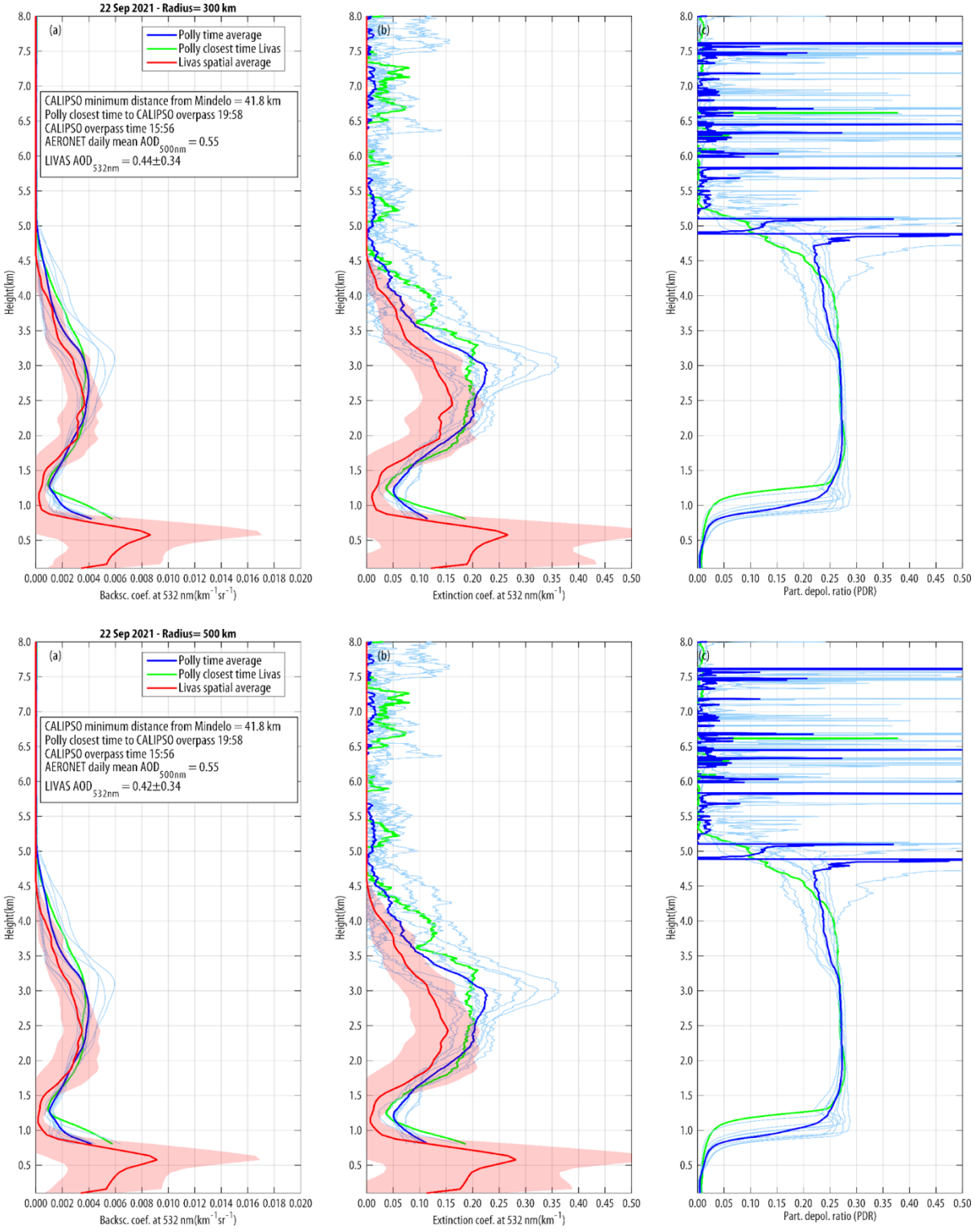

Figure 6: Comparison of the LIVAS at (100 km, 300 km, and 500 km) and Pollyxt profiles of (a) backscatter coefficients, (b) extinction coefficient, and (c) vol.depolarization.ratio for the 22 September 2021, considering (pure dust).

Figures 7 and 8 present the mean backscatter and extinction coefficient profiles for September 2021 over Mindelo as evaluated by LIVAS (for different radii) and PollyXT. For Figure 7 the

mean values are obtained by considering only profiles that Polly is collocated with LIVAS, and Figure 8 consists of an average considering all profiles of each product. Unarguably for both cases, and for all radii, there is an excellent agreement between Polly and LIVAS profiles at a monthly scale. Nevertheless, the greater the radius the better the agreement, which can be attributed to statistical improvement from the LIVAS side as the number of CALIPSO overpassing increases. Despite its specific location, at Mindelo city, this also shows Polly spatial representativity at the monthly scale, which is vital for regional climatological studies.

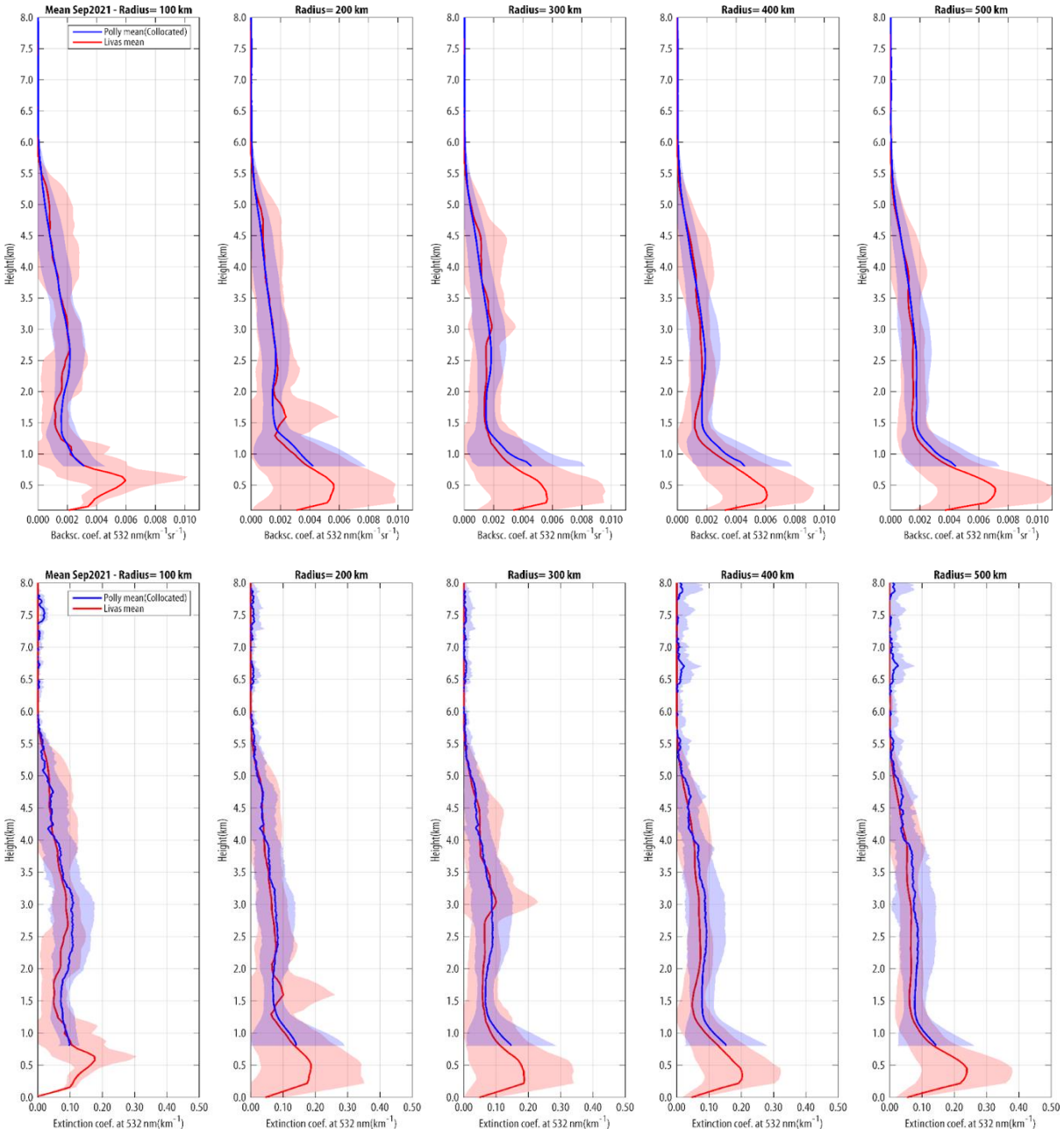

Figure 7: Mean backscatter (top) and extinction(bottom) coefficient profiles of LIVAS (as function of radius) and PollyXT for September 2021 over Mindelo city considering collocated profiles (for the same day).

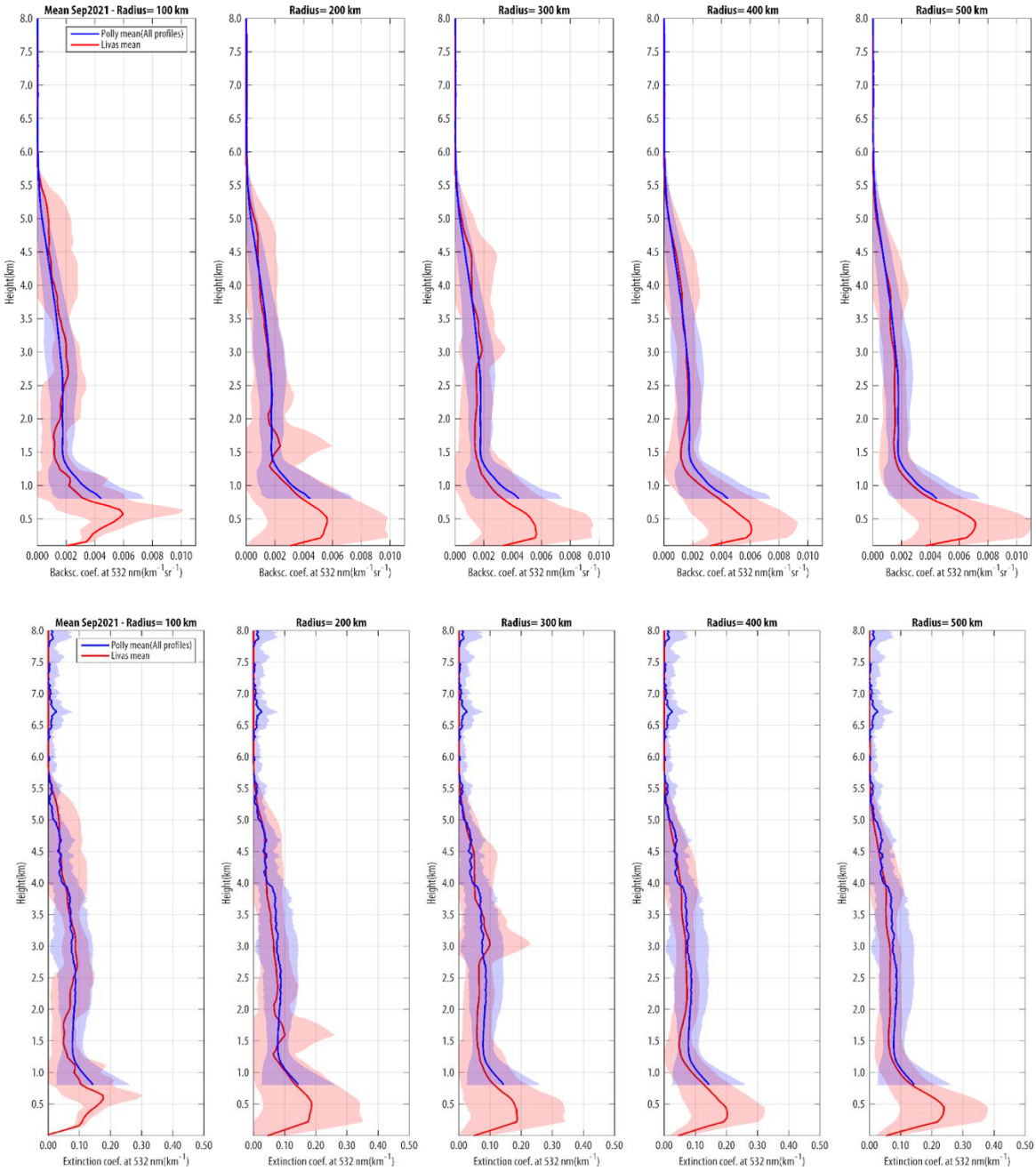

Figure 8: Mean backscatter (top) and extinction (bottom) coefficient profiles of LIVAS at all radius and Pollyxt profiles considering all days of September 2021(for PollyXT).

4.2. All aerosols and dust climatology over Mindelo.

This section performed a climatological characterization of seasonal variability of all aerosols and pure dust profile and optical depth over the eastern tropical Atlantic based on LIVAS long-term data centered at Mindelo city, Cape Verde. The climatology will be based on period spans from 2006-2021. The analysis and results obtained are based on the following LIVAS-provided optical properties: Aerosol Optical Depth (AOD), Dust Optical Depth (DOD), backscatter, and

extinction coefficient profiles all at 532 nm. This investigation explores their typical monthly and seasonal variability and the interannual variation of AOD and DOD from 2006 to 2021.

Figure 9 presents LIVAS profiles monthly frequency as a function of radius, centered on Mindelo, and year. As the radius increases from 100 km to 500 km, the frequency of profiles per month substantially increases. For the smallest radii (100 km), the maximum number of the profiles obtained was 6. For 500 km, the number increases to 25 profiles particularly the radius 500 km, presenting a notably higher number of profiles. The increased in radius leads to coverage of larger CALIPSO overpassing, meaning that LIVAS will have more profiles. This can impact the representativity of LIVAS monthly means, especially to smaller radii (100 and 200 km) that have a small number of profiles per month. Certain months and years have zero profiles for all radius. Specifically, there are zero profiles for January to June 2006, February 2016, September 2019, and January to February 2021, indicating a lack of measurements during these periods.

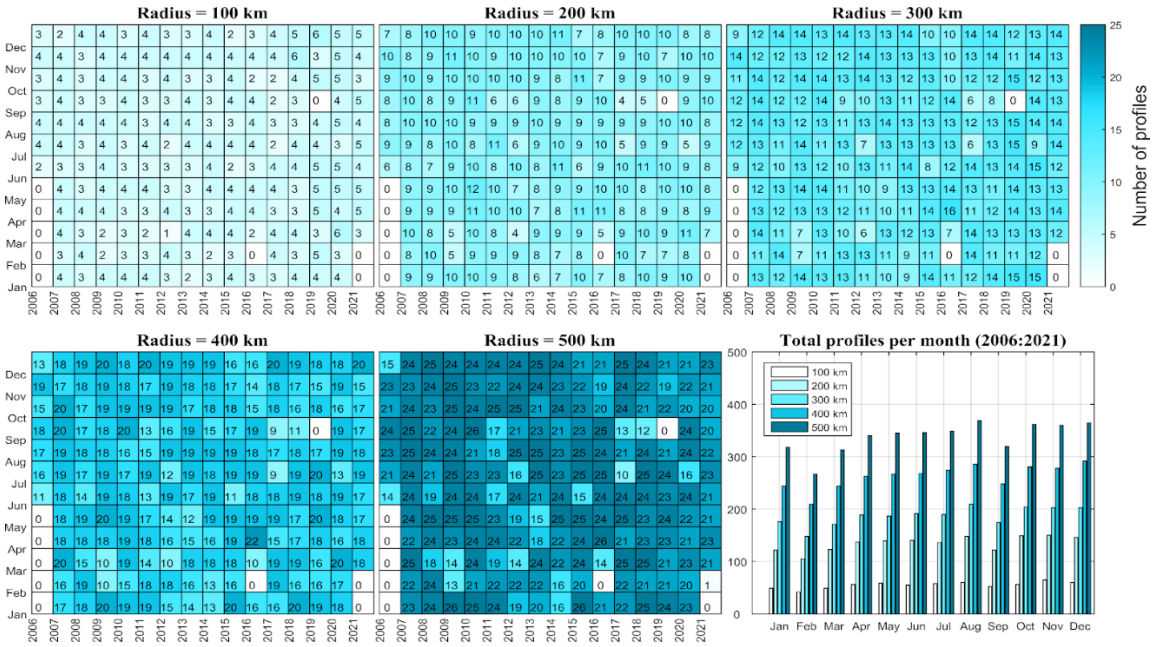

Figure 9: LIVAS profiles frequency as a function of radius centered on Mindelo city, month and year from 2006 to 2021.

4.2.1. All aerosol and dust Optical Depth annual cycle.

Figure 10 shows simultaneously the annual cycle and inter-annual variability of AOD, based on monthly mean, from 2006 to 2021 per radius centered at Mindelo. The AOD over all radii domains starts to increase around May (~0.4), peaks during June (~ 0.6), and July, and then starts to decrease until October (~0.3), when values lower than those observed in May are

registered. This feature is consistently represented by all aggregation radii and it is supported by the results of the AERONET long-term site in Cabo Verde located at Sal Island. However, as the radius increases from 100 km to 500 km AOD values get diluted, mainly during aerosol season peak (June, July, August), high values ($AOD_{532\,nm}$ > ~0.8) become less frequent, but so become clean conditions ($AOD_{532\,nm}$ < ~0.3). A possible explanation for this behavior is that with a smaller redius (100 km), not all Saharan dust plumes traveling toward the Atlantic would be captured by the smaller radius domain. Therefore, producing at times, a clean scenario and other times moderate or highly polluted conditions when vigorous plumes cross the smaller redius. However, as the radius increases it is very likely an increase in frequency of dust plumes leaving North Africa being sampled within this radius, which would produce a different pattern of monthly AOD distribution, more diluted but higher than typical background in dust absence. Nevertheless, CALIPSO overpassing frequency as a function of radius might play a role on the AOD observed features. This analysis of the monthly mean of also AOD shows that there is less aerosols over Cape Verde from January to April, with $AOD_{532\,nm}$ varying roughly from 0.2 to 0.3. The largest variability is observed from May to October, with a peak in June between 0.6 to 0.7, and a decrease from November to December. Regarding the interannual variability, minimum AOD values were observed during the years 2011 and 2015, while an example of high AOD years 2012 and 2018 can be highlighted.

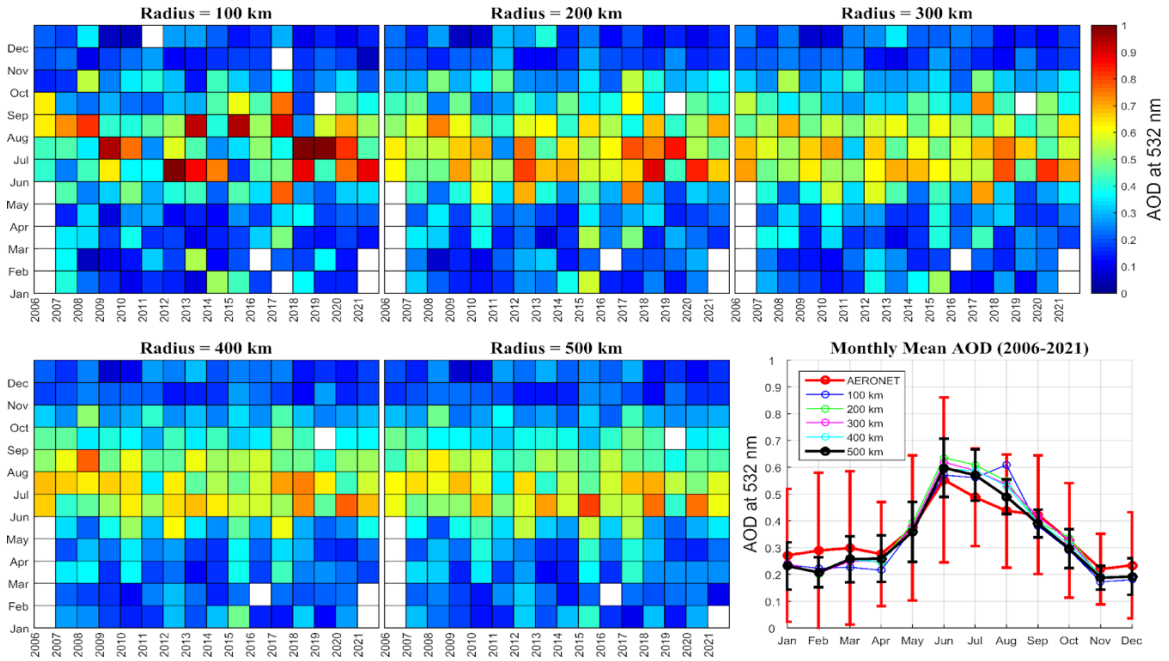

Figure 10: LIVAS annual cycle and inter-annual variability of AOD532 nm over different radius centered at Mindelo city, Cabo Verde, from 2006 to 2021. On the right-bottom corner is presented the climatological annual

cycle of AOD532nm as obtained from LIVAS using the different radius and AERONET long-term dataset from the Sal Island sunphotometer.

Figure 11 shows the annual cycle and inter-annual variability of Dust Optical Depth (DOD) over Mindelo from 2006 to 2021 per month and per radius. Climatological monthly mean cycle of DOD is also presented for the different radii. DOD seasonal patterns resemble AOD features, which shows that the seasonality of AOD over the analyzed region is mainly driven by dust transport. Most of the dust over Mindelo is observed from May to October, as is the case of AOD. The monthly mean of DOD shows that for all radius there is high transport during this period. As for the AOD, there is a prominent peak of DOD in June between 0.3 to 0.4 nm, at least for the radii of 500 km, 400 km, and 300 km, and between 0.2 to 0.3 nm for a radius of 200 km. The radius of 100 km displays the lowest DOD, with a peak around 0.2. At the radius of 100 km, there are few monthly high DOD scenarios in 2008, 2012, 2013, and 2019. As the radius increases, from 200 km to 500 km, there is enhancement in DOD mainly during June, July and August.

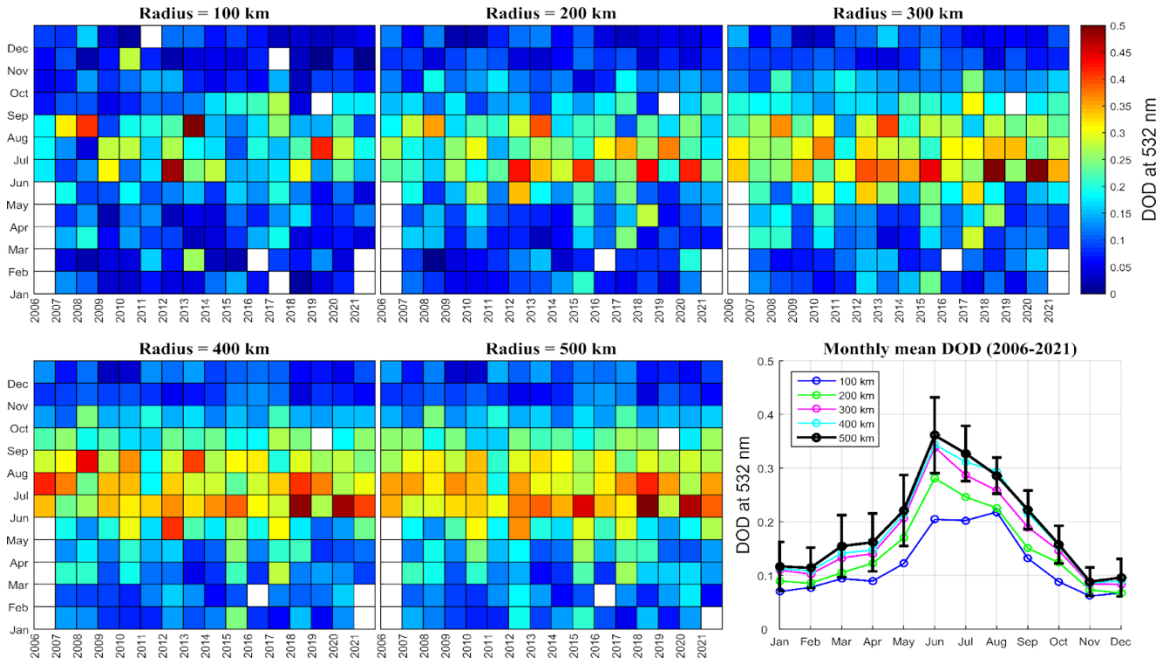

Figure 11: LIVAS annual cycle and inter-annual variability of DOD532 nm over different radius centered at Mindelo city, Cabo Verde, from 2006 to 2021. On the right-bottom corner is presented the climatological annual cycle of DOD532nm as obtained from LIVAS using the different radius

4.2.2. All aerosols and Dust backscatter and extinction profiles.

Figure 12 shows the mean annual cycle of the aerosol backscatter and extinction coefficient profiles at 532 nm for the distinct radii centered on Mindelo, considering the period from 2006

to 2021. The main vertical feature of aerosol profile over the studied domain, which is present in all radii, is the strong seasonality in aerosol loading in the free troposphere just above the Marine Boundary Layer (MBL, ~ above 1 km). For all radius, in the free troposphere, there are fewer aerosols from January to May and a higher amount from June to November a peak in September to October between 2.5 and 3.5 km where aerosols are transported above the boundary layer. As can be confirmed in Figure 22, this feature is a direct response to the Saharan dust transport seasonality. There is a significant amount of aerosols in the MBL round year.

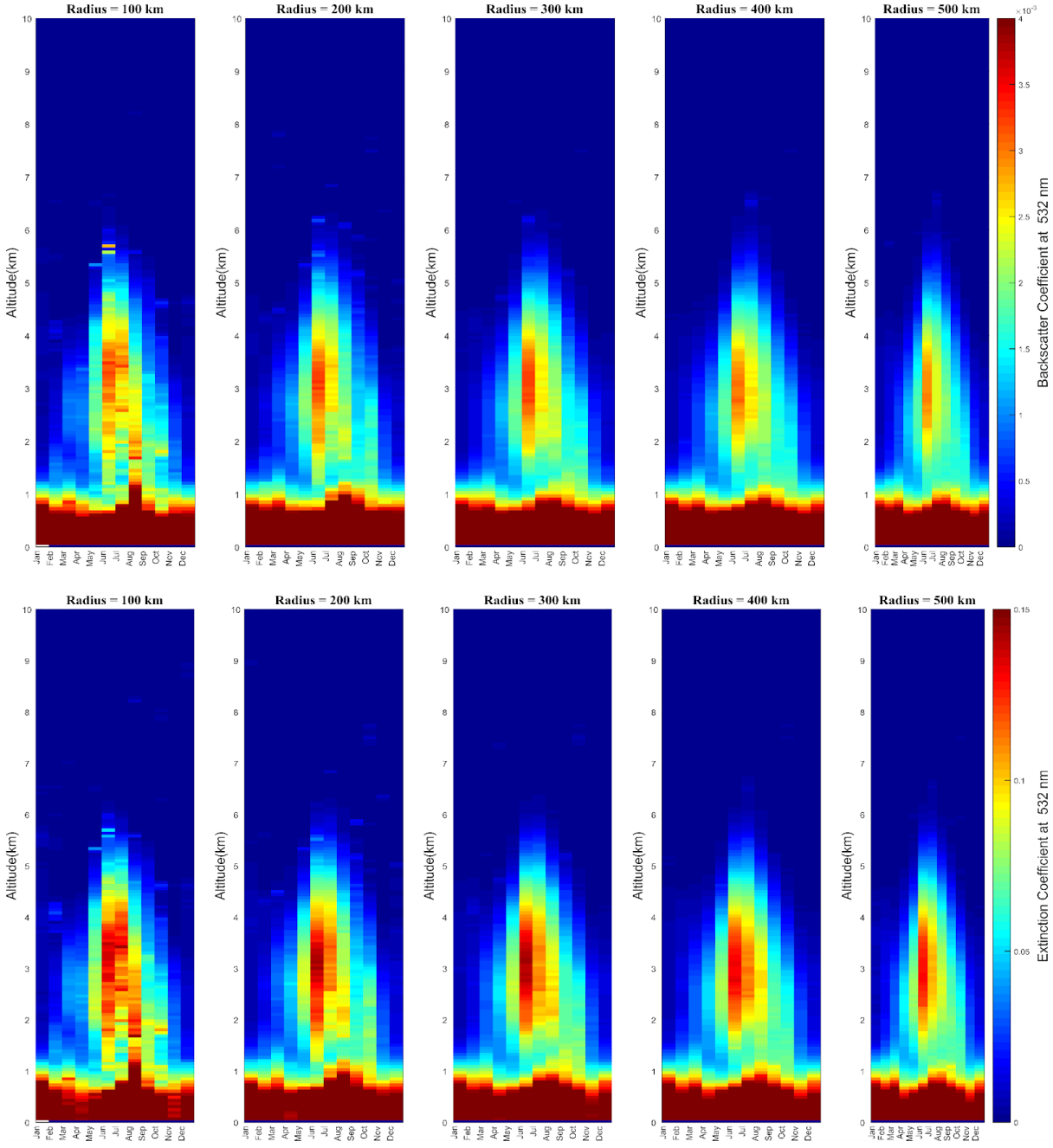

Figure 12: Mean annual cycle of the all aerosols backscatter (top) and extinction (bottom) coefficient profiles at 532 nm per radius centered at Mindelo as derived from LIVAS aerosol products from 2006 to 2021.

Figure 13 shows the annual cycle mean of the backscatter and extinction coefficient profiles specifically for pure dust. For all radii, dust transport over Cape Verde is particularly intense at layers between 2 km and 4 km from June to December.

Within MBL, is it possible to also identify a seasonality in aerosol loading. Less aerosols close to the surface from March y to June. There are peaks in dust abundance close to the surface during the winter (DJF), indicating the predominance of low-level transport of Saharan dust. Apart from these periods, pure dust is reduced, suggesting other aerosol types also drive particle abundance seasonality close to the surface.

The analysis of all the radii of 100 km, 200 km, 300 km, 400 km, and 500 km revealed a similar pattern, which indicates consistent seasonal characterization of all aerosols and dust distribution by the radii assumptions.

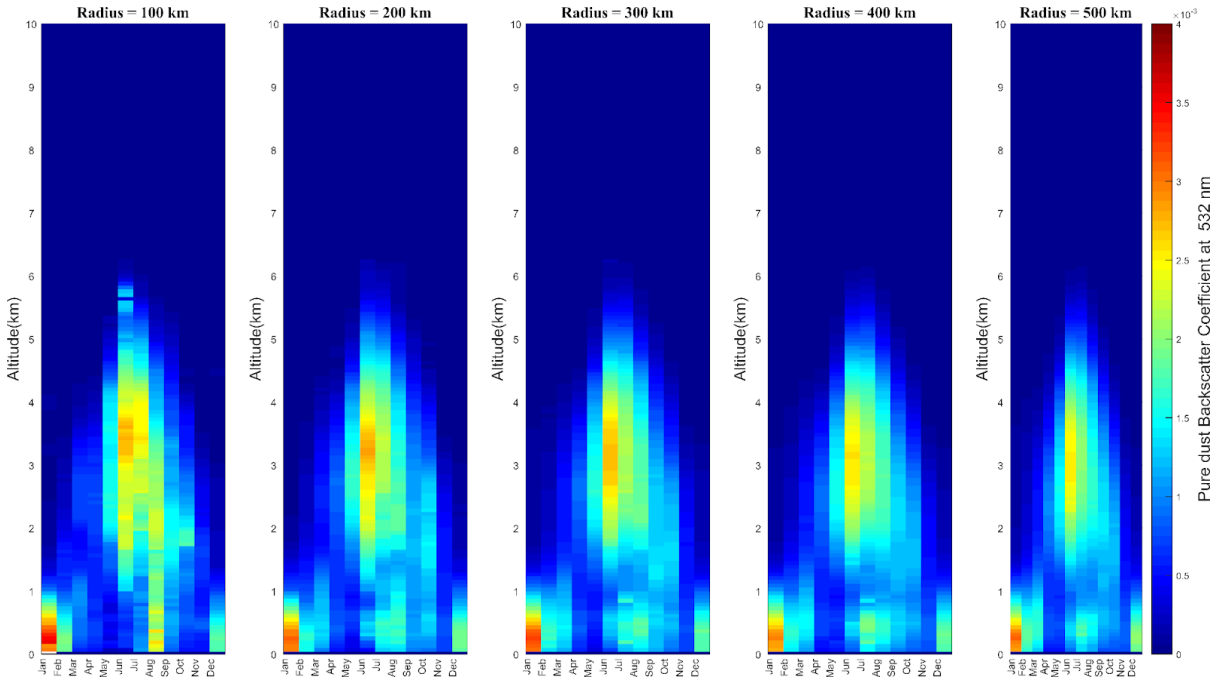

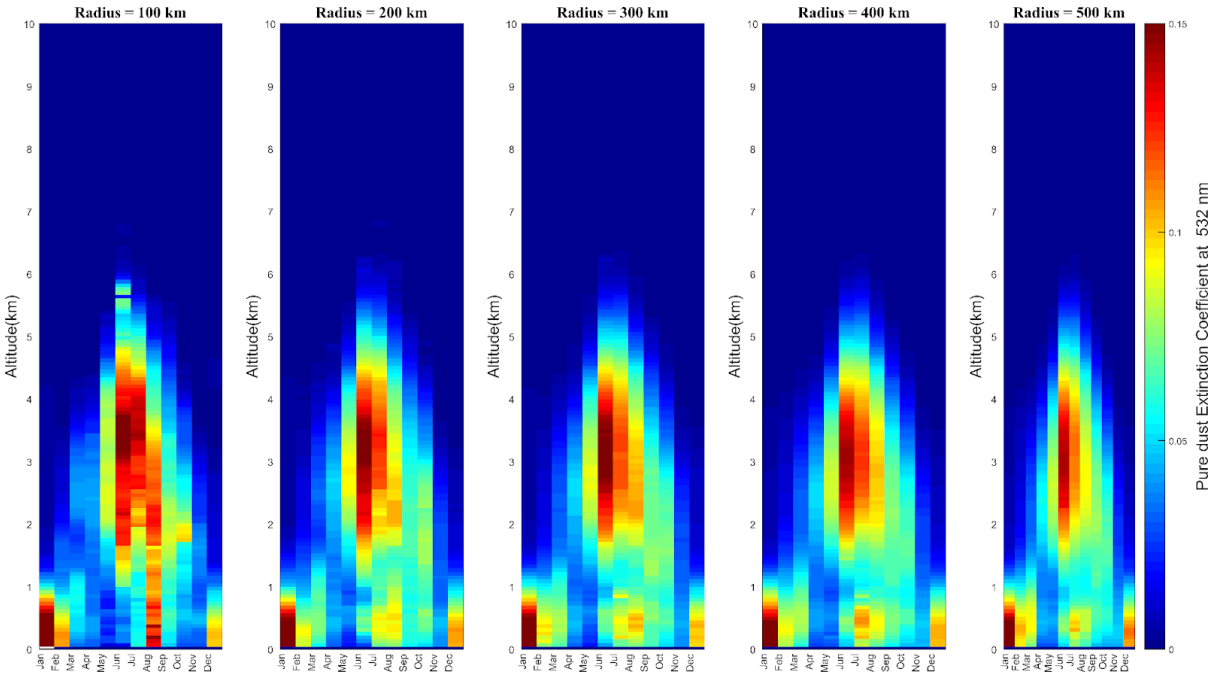

Figure 13: Mean annual cycle of the pure dust backscatter (top) and extinction (bottom) coefficient profiles at 532 nm per radius centered at Mindelo as derived from LIVAS aerosol products from 2006 to 2021.

Figure 14 presents the seasonal climatology of vertical distribution of all aerosols and pure dust over Cabo Verde, respectively, derived by LIVAS. The results are presented in terms of mean, median and standard deviations.

As seen previously, the main aspect of the aerosol structure over the study region is the strong seasonality in the free troposphere, with summer and winter standing on opposite sides. During the summer season, there is a significant increase in aerosols in the layers above Marine boundary Layer, peaking between 2 and 4 km. This is explained by the Saharan dust transport (Figure 27). The close values between mean and median at these altitudes indicate that dusty air masses are frequent. From autumn, there is a decrease in aerosols, with the free troposphere reaching a minimum during boreal winter, when Saharan dust transport at higher levels is reduced. During winter, most of the aerosols are confined to the MBL, dust transport plays a role, as can be seen in the pure dust profile in winter, but it would explain just a fraction of the aerosols present in the MBL. All radii consistently represent these behaviors; however, for 100 km a larger variability (standard deviation) and difference between mean and median are seen. This can be explained by the reduced number of LIVAS profiles obtained for this radius when compared with 300 and 500 km.

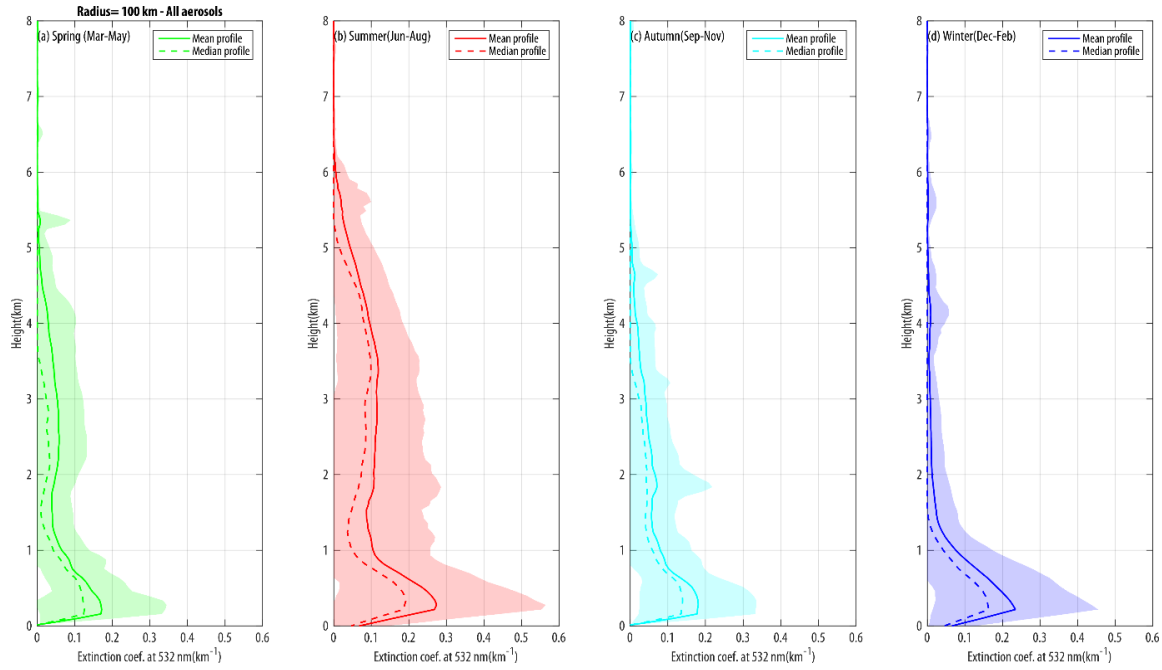
Radius= 100 km - All aerosols
(a) Spring (Mar-May)
(b) Summer(Jun-Aug)
(c) Autumn(Sep-Nov)
(d) Winter(Dec-Feb)
Mean profile
Median profile
Height(km)
Extinction coef. at 532 nm(km^{-1})

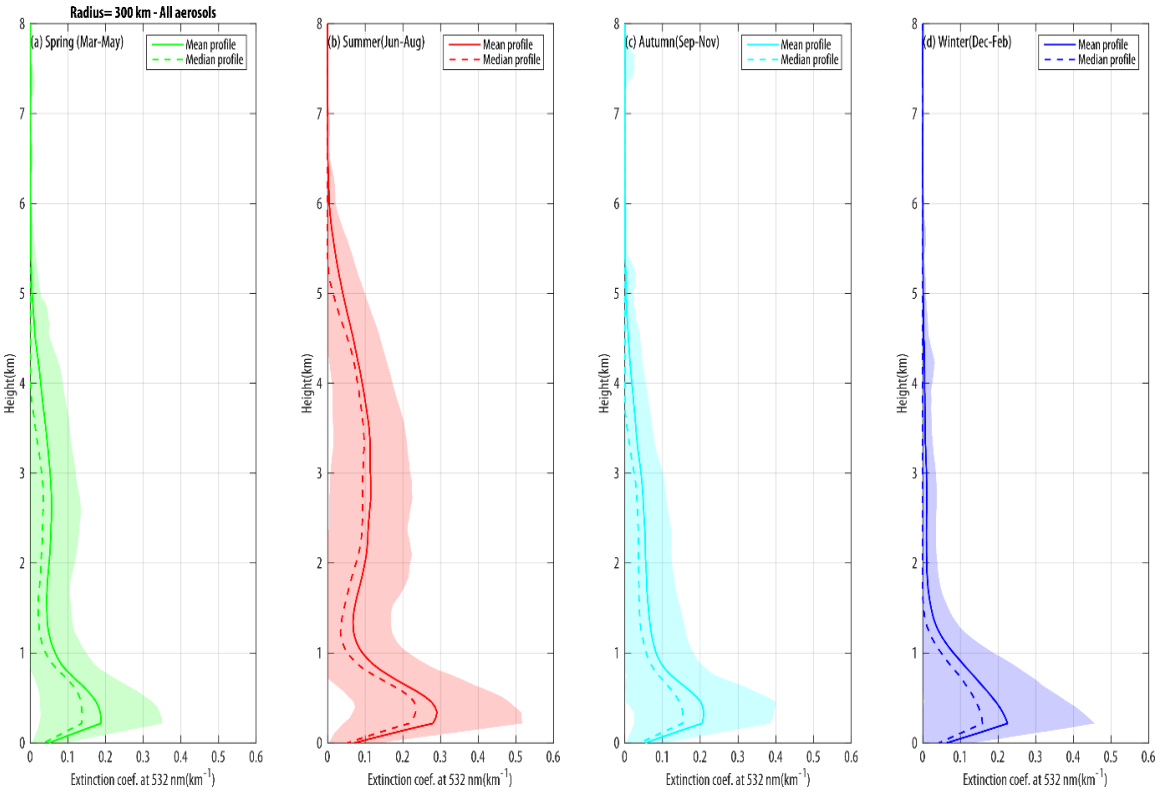
Radius= 300 km - All aerosols
(a) Spring (Mar-May)
(b) Summer(Jun-Aug)
(c) Autumn(Sep-Nov)
(d) Winter(Dec-Feb)
Mean profile
Median profile
Height(km)
Extinction coef. at 532 nm(km^{-1})

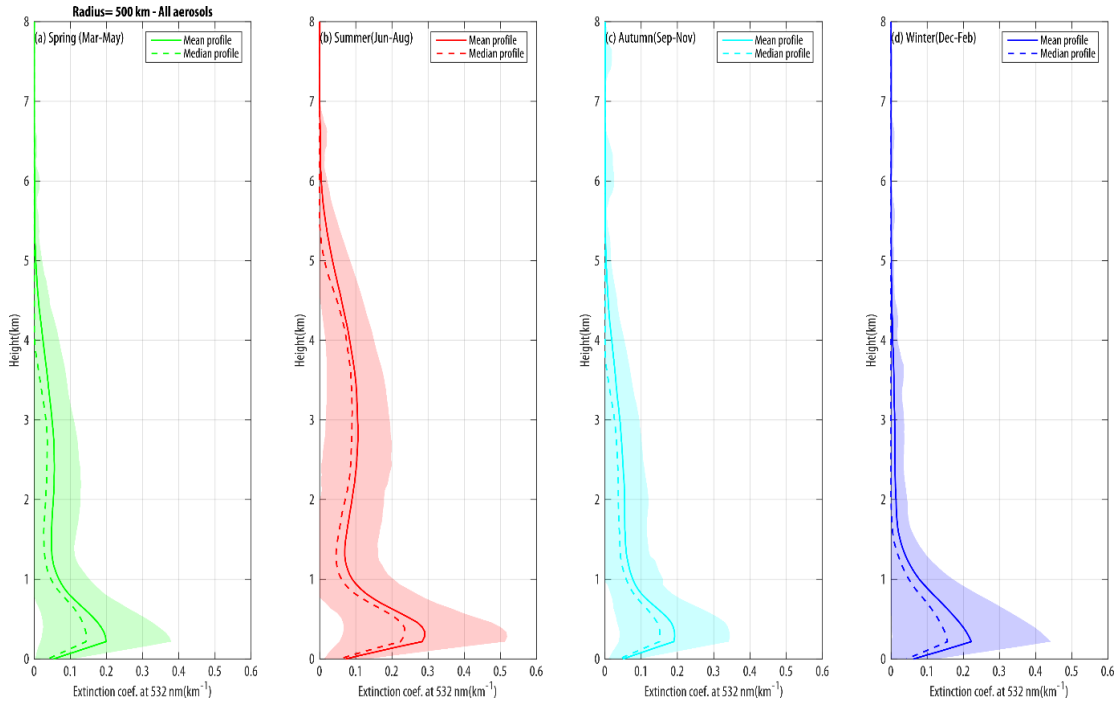

Figure 14: Seasonal variation of all aerosol extinction coefficient profiles at 532 nm as a function of radius centered at Mindelo as derived from LIVAS aerosol products from 2006 to 2021. Top panel (100 km), Middle panel(300 km), bottom panel (500 km).

The pure dust profiles show that in (Fig. 15 100 km, 300 km, and 500 km) there is transport of Saharan dust throughout the seasons over Cabo Verde, most of the time (summer, spring and autumn) these dust plumes are traveling aloft. Only during the winter that the transport is mostly confined to the MBL. However, even during summer, spring and autumn, dust also occurred at levels close to the surface.

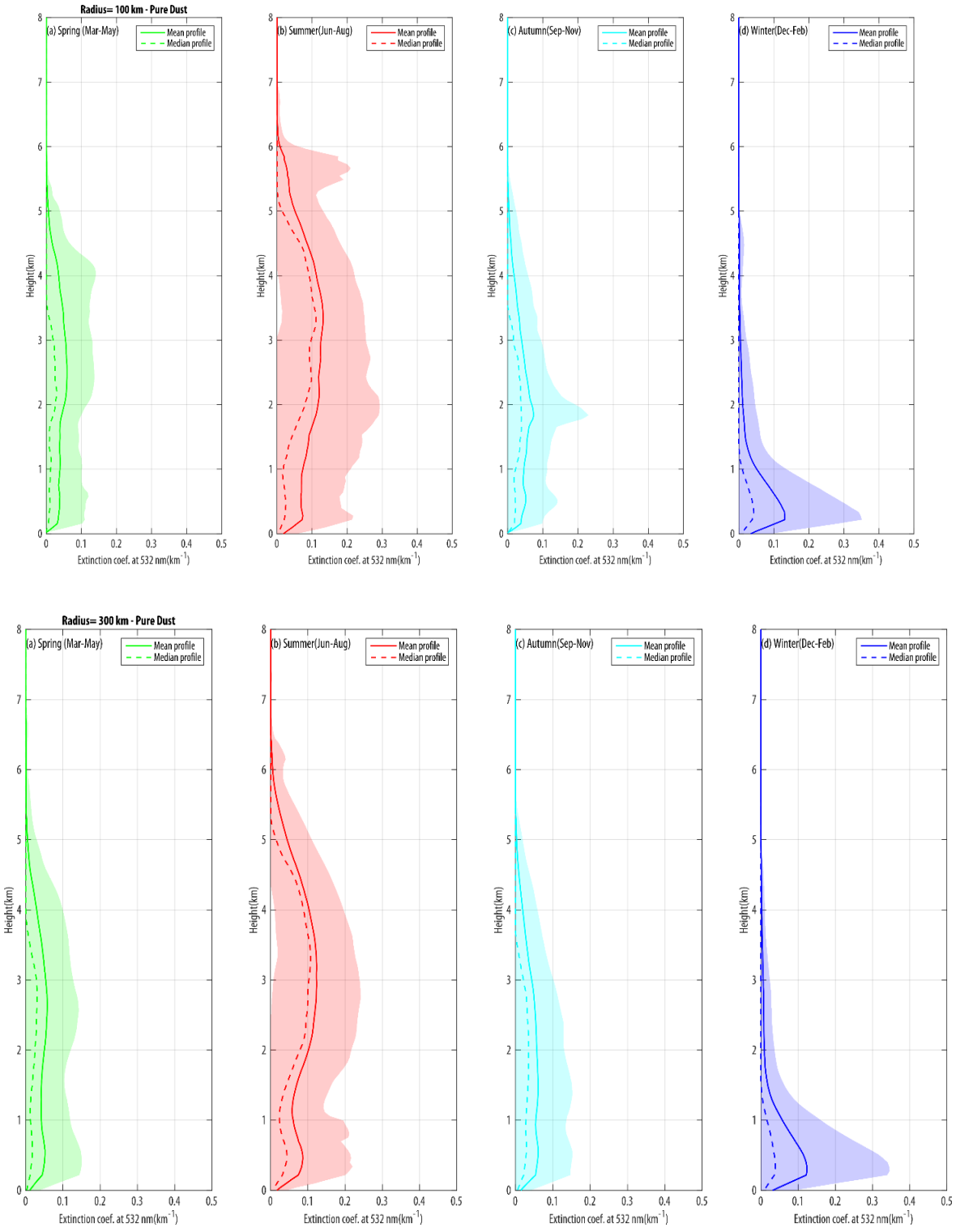
Radius= 100 km - Pure Dust
(a) Spring (Mar-May)
(b) Summer(Jun-Aug)
(c) Autumn(Sep-Nov)
(d) Winter(Dec-Feb)
Mean profile
Median profile
Height(km)
Extinction coef. at 532 nm(km-1)
Radius= 300 km - Pure Dust
(a) Spring (Mar-May)
(b) Summer(Jun-Aug)
(c) Autumn(Sep-Nov)
(d) Winter(Dec-Feb)
Mean profile
Median profile
Height(km)
Extinction coef. at 532 nm(km-1)

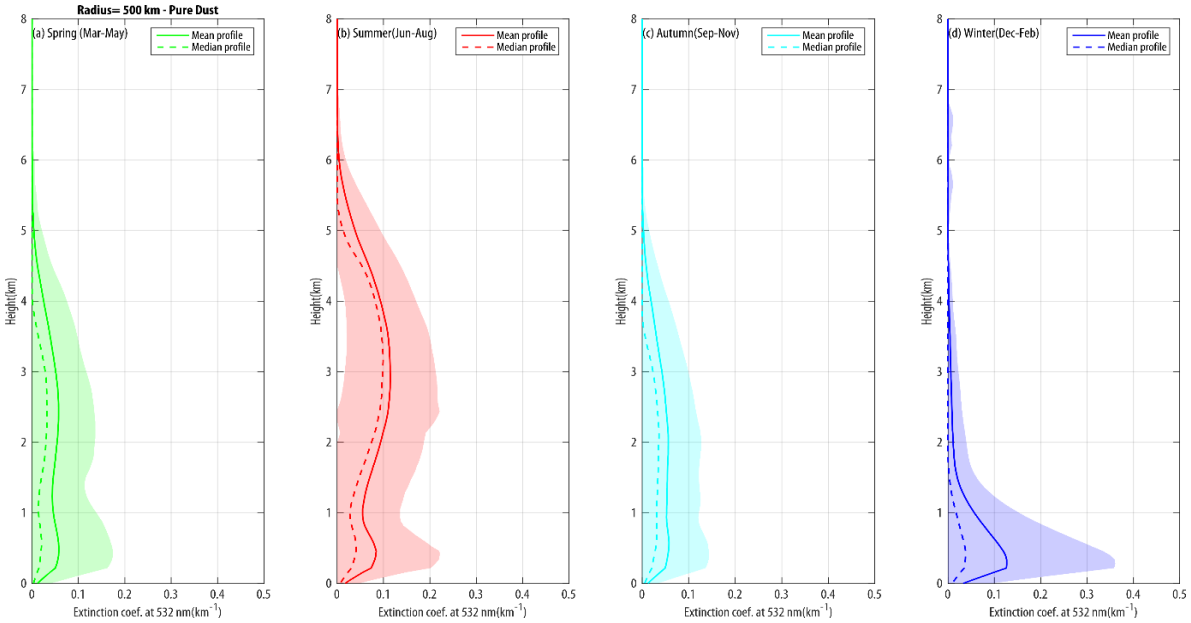

Figure 15: Seasonal variation of dust extinction coefficient profiles at 532 nm as a function of radius centered at Mindelo as derived from LIVAS aerosol products from 2006 to 2021. Top panel (100 km), Middle panel (300 km), bottom panel (500 km).

Figure 16 presents the seasonal variation of the dust fraction as regard to the backscatter and extinction coefficient profiles for the different radii. It describes the relative contribution of dust to the aerosol's extinction of solar radiation in the visible spectrum (532 nm). The dust fraction increases significantly with altitude, for all radii, in the summer. In the free troposphere, between 1.5 and 6.0 km, dust responds by almost 100% of the extinction during summer. Similar behavior is seen for spring and autumn, but above 5 km dust, contribution starts to decrease. During the winter, dust contribution decreases gradually from ~100%, just above the MBL, to less than 50% above 4 km. Within the MBL dust contribution decreases gradually as it gets closer to the surface to a value below than 25%. As expected, the larger contribution at the surface is seen during the boreal winter. In general, these features within MBL are consistent among the radii. The main difference is observed at the radius of 100 km which estimates a larger contribution of dust when compared to the other radii.

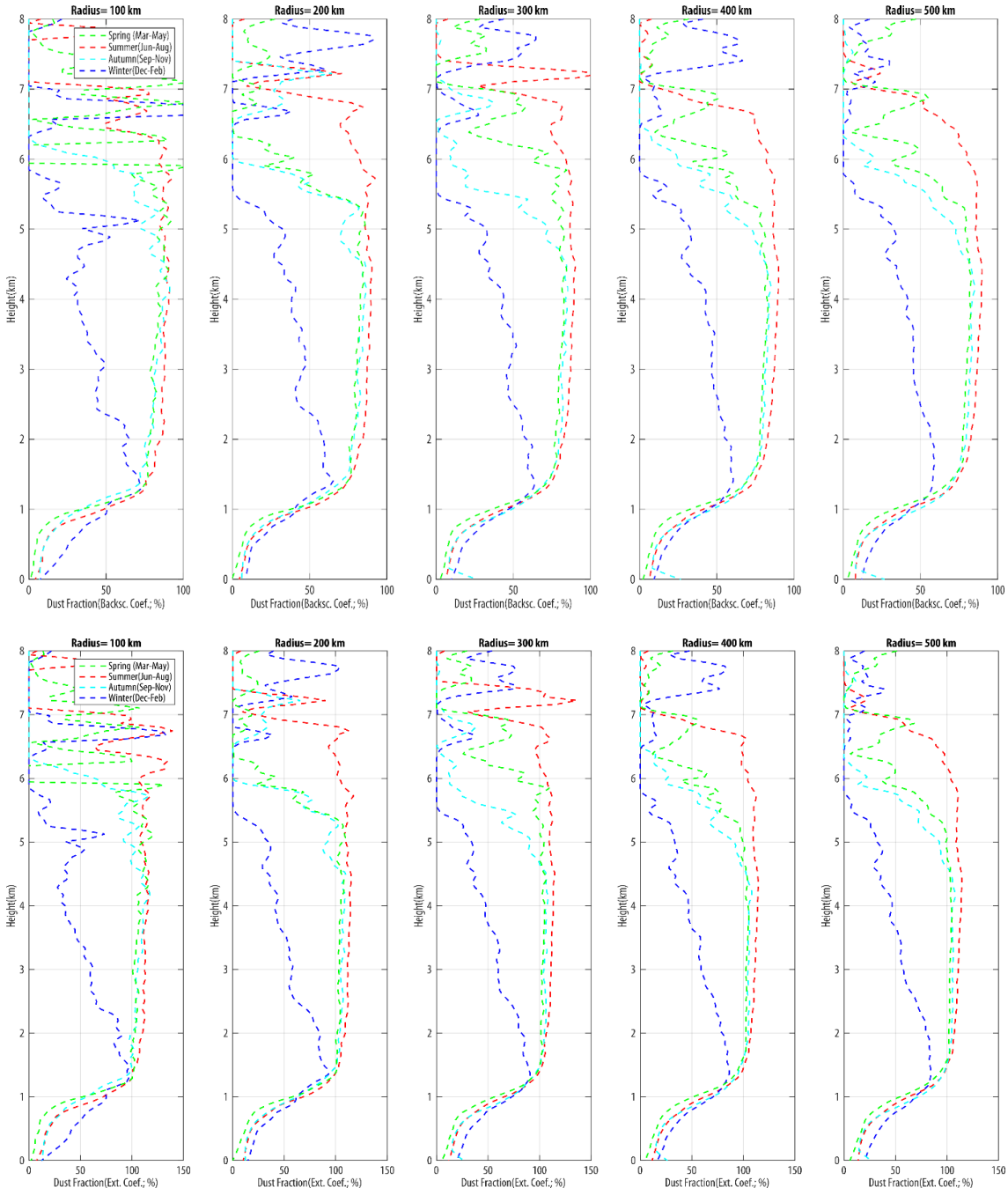

Figure 16: Seasonal variation of dust relative fraction as regard to the backscatter(top) and extinction(bottom) coefficient profiles at 532 nm and as a function of radius centered at Mindelo derived from LIVAS aerosol products from 2006 to 2021.

4.3. Saharan dust transport to the tropical Atlantic: Annual and Seasonal mean structure

This section provides a characterization of the annual and seasonal mean horizontal and vertical structure of all aerosols and pure dust transport to the Tropical Atlantic and the Americas as described by LIVAS long-term climatology. Figure 17 presents the annual mean horizontal

structure of all aerosols and pure dust as described by AOD at 532 nm. The pure dust field reveals LIVAS ability to isolate dust from the other aerosol types. Over North Africa, DOD reaches overspread values as high as 0.4 for the annual mean. The pattern of dust transport towards the tropical Atlantic and Americas is shown in Fig. 17.

The annual DOD indicates high transport closer to the North African coast in the Eastern Tropical Atlantic domain (DOD532nm ~ 0.3), and a gradual decrease as the plume reaches the Americas (DOD532nm ~ at 0.1).

Results are also presented as transects of latitude-altitude of extinction coefficient profile at 3 specific longitudes (24.5^{o}; 40.5^{o} and 60.5^{o}) for both all aerosols and pure dust, and also for the transect of dust fraction in Fig. 18. This reference's longitudes are respectively, taken observing Mindelo city, a point elsewhere in the middle of the Atlantic and Manaus, the Amazonia state capital. The vertical structure of the averaged coefficient for all aerosols along Mindelo longitude reveals an aerosol layer extending from north to south in the MBL and another layer above extending up to 5 km and with a core between 2 and 3 km and restricted to the latitudes between 10^{o}N and 20^{o}N. Isolating the pure dust extinction coefficient and determining its contribution to the extinction (dust fraction), the results show that the aerosol layer aloft is dominated by dust (almost 100%) while dust relative contribution in the MBL is significantly lower (<50%). Nevertheless, the dust annual average of the extinction coefficient over Mindelo longitude is higher at lower levels than in the free troposphere. The further away references longitudes show that the dust is always ubiquitous all the way until the Americas, however is drastically reduced. Nevertheless, dust fraction keeps explaining most of the aerosols' extinction effects above MBL (~100 %). In terms of value, extinction coefficient of pure dust varied from a high value 0.08 km-1 close to the surface at Mindelo longitude to less than 0.03 km^{-1} in the north part of South America and at Manaus longitude reference.

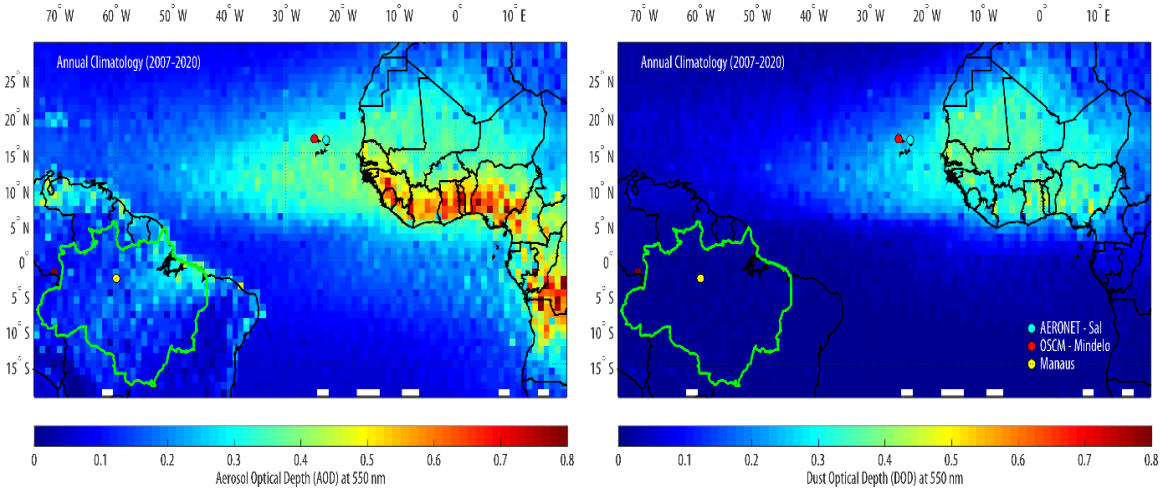

Figure 17: Annual climatology of Aerosol Optical Depth (AOD) and Dust Optical Depth (DOD) at 532 nm based on LIVAS aerosol product for the period between 2007 and 2020. The circles markers on the maps indicate the city of Mindelo (red), taken as the reference of the OSCM coordinates, the Sal Island (cyan), and Manaus city (yellow), the capital of Amazonia states as a reference for South America.

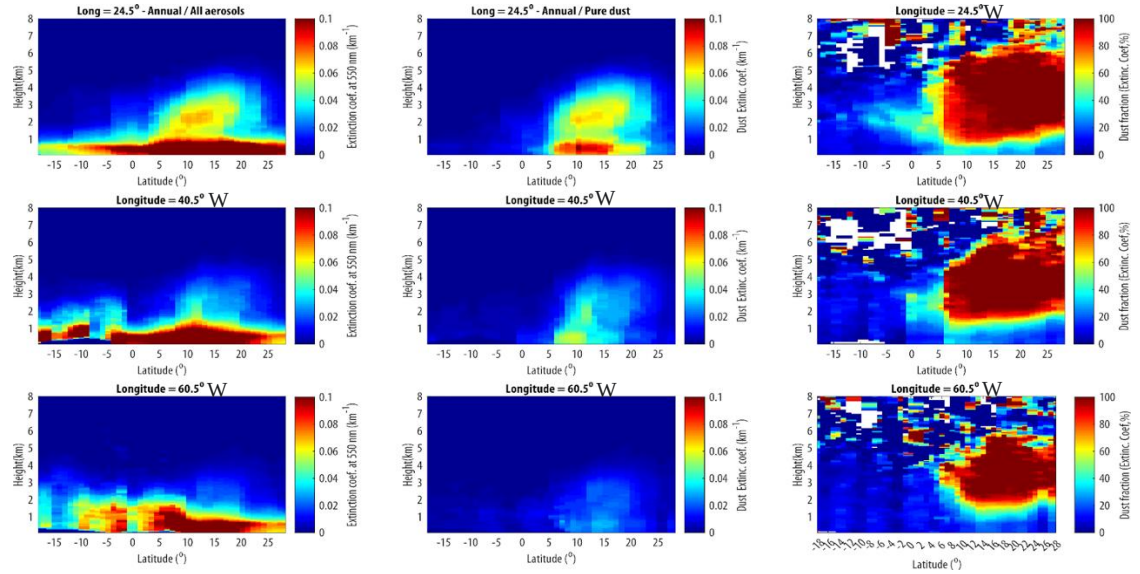

Figure 18: Extinction coefficient and dust fraction profiles as latitudes transects at references longitude: this allows us to see the vertical transport structure at different longitude (close to Mindelo, Cape Verde, in the middle of the Atlantic and close to Mindelo, Cape Verde, in the middle of the Atlantic and close to Manaus longitude, Amazonia)

Figure 19 shows the mean horizontal structure of all aerosols and pure dust transport toward the tropical Atlantic during the spring season. High AOD values (up to 0.8) are seen from central to western of Sahara. The plume core is traveling south of Cabo Verde toward the northern part of South America. It is worth mentioning LIVAS product effectiveness to remove Africa biomass burning aerosol from the pure dust product. DOD also shows high values across the Sahara domain (up to 0.7). South of over Cabo Verde, dust plume optical depth

decreases to values between 0.4 and 0.5, until reaching South America the plume presents DOD lower than 0.3.

The latitude-altitude transect results (Fig. 20) show the vertical and latitudinal distribution of dust extinction coefficient for all aerosols and pure dust alongside dust fraction along the reference longitudes during spring. For all aerosols, one can see high dust extinction values close to the surface (0.1 km^{-1}) for all reference longitudes. However, the Saharan plume leaving North Africa is clearly depicted over Mindelo reference longitude. From the pure dust transect it is possible to see that the plume, at its lower boundary, is restricted to a latitude between 5º and 15º, while at higher levels, it extends until 25º. As it moves eastward, the plume is significantly diluted and confined to 5º and 15º in its vertical extension. The pure dust extinction coefficient profile along Mindelo longitude reference indicates the highest values are observed at high altitudes between 2 and 5 km the dust fraction responds up to 100% of the extinction coefficient, in the MBL it responds to less than 30%.

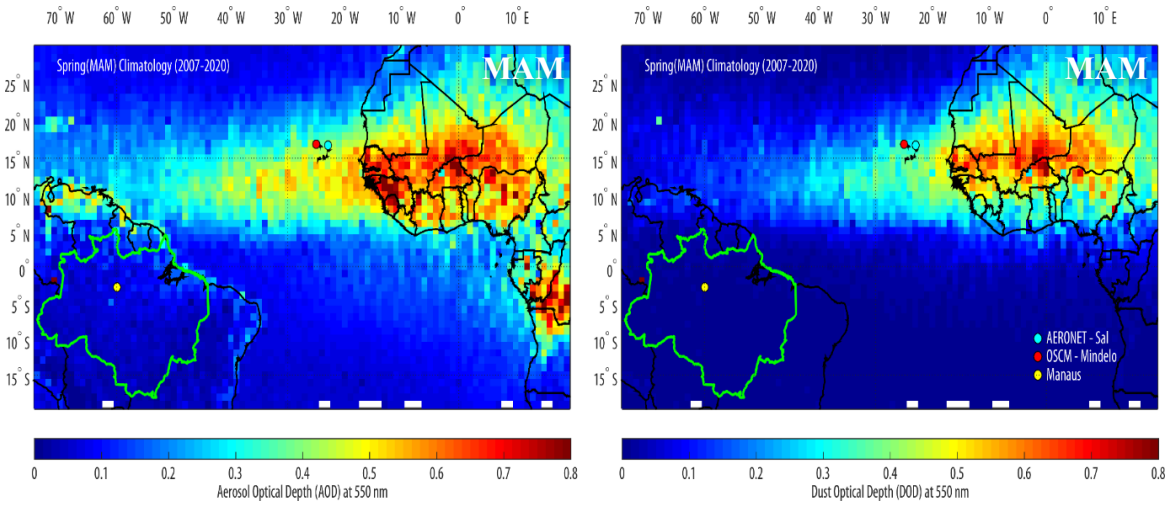

Figure 19: Boreal spring (March - April - May) climatology of Aerosol Optical Depth (AOD) and Dust Optical Depth (DOD) at 532 nm based on LIVAS aerosol product for the period between 2007 and 2020. The circles markers on the maps indicate the city of Mindelo (red), taken as the reference of the OSCM coordinates, the Sal island (cyan) and Manaus city(yellow), the capital of Amazonia states as a reference for South América.

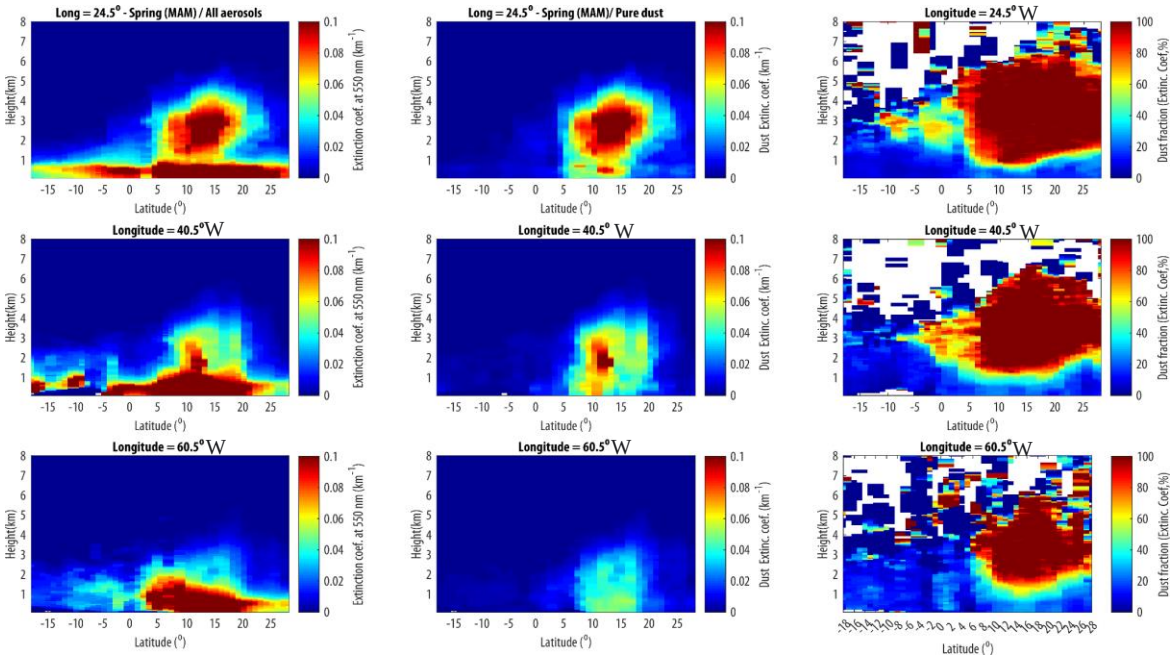

Figure 20: Boreal spring (March - April - May) mean of the latitude-height transect of extinction coefficient (for all aerosols and pure dust) and dust fraction (as a relative contribution to the total extinction coefficient) for three longitudes of reference: Mindelo city (24.5º), Cabo Verde, as a reference to the structure when Saharan dust leave North Africa, elsewhere in the middle of the Atlantic (40.5º) and Manaus city (60.5º), the capital of Amazonia states, in the northern region of South America.

Figure 21 shows that during the summer period, Saharan dust is transported to the tropical Atlantic travelling at the center and north of Cabo Verde. It moves predominantly to the central and north region of America. This northward displacement in the plume is forced by the ITCZ northward movement, which leaves regions further south of Cabo Verde relatively free of the plume effect. Over the Sahara, high AOD values (up to 0.8) are seen displaced to its north portion when compared to the spring season. DOD varies from ~ 0.7 across the northern part of the saharan desert to around 0.3 in the middle of the tropical Atlantic and less than 0.2 in Caribbean and Central America.

The extinction coefficient transects (Fig. 22) show the Saharan plume leaving North Africa with its core around 3 km and in its most northward position between latitudes 10º and 25º. Extinction coefficients are high (up to 0.1 km^{-1}, all aerosols) close to the surface for all transects. The layer of aerosol south of the Equator (-5º to -15º) related to biomass burning in South America presents its depth from the surface up to 3 km. As the dust plume moves toward America its intensity decreases as the remotion and deposition take place. Nevertheless, it is possible to find dust in all layers, from MBL to the free troposphere, in the remote region of

Central America. However, as the extinction coefficient profile shows, most of the pure dust is transported in upper layers at high altitudes (2-5 km)

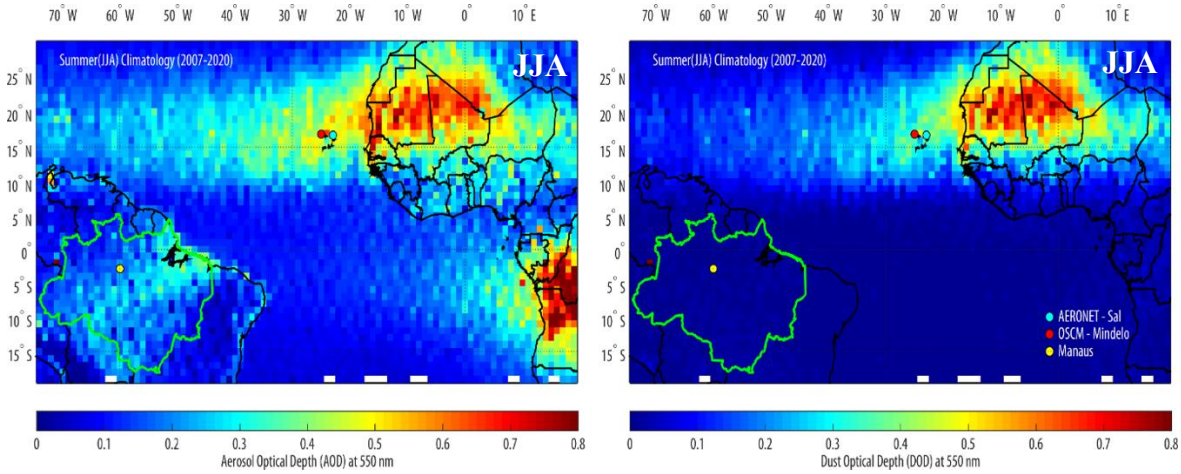

Figure 21: Boreal summer (June - July - August) climatology of Aerosol Optical Depth (AOD) and Dust Optical Depth (DOD) at 532 nm based on LIVAS aerosol product for the period between 2007 and 2020. The circles markers on the maps indicate the city of Mindelo (red), taken as the reference of the OSCM coordinates, the Sal island (cyan) and Manaus city(yellow), the capital of Amazonia states as a reference for South América.

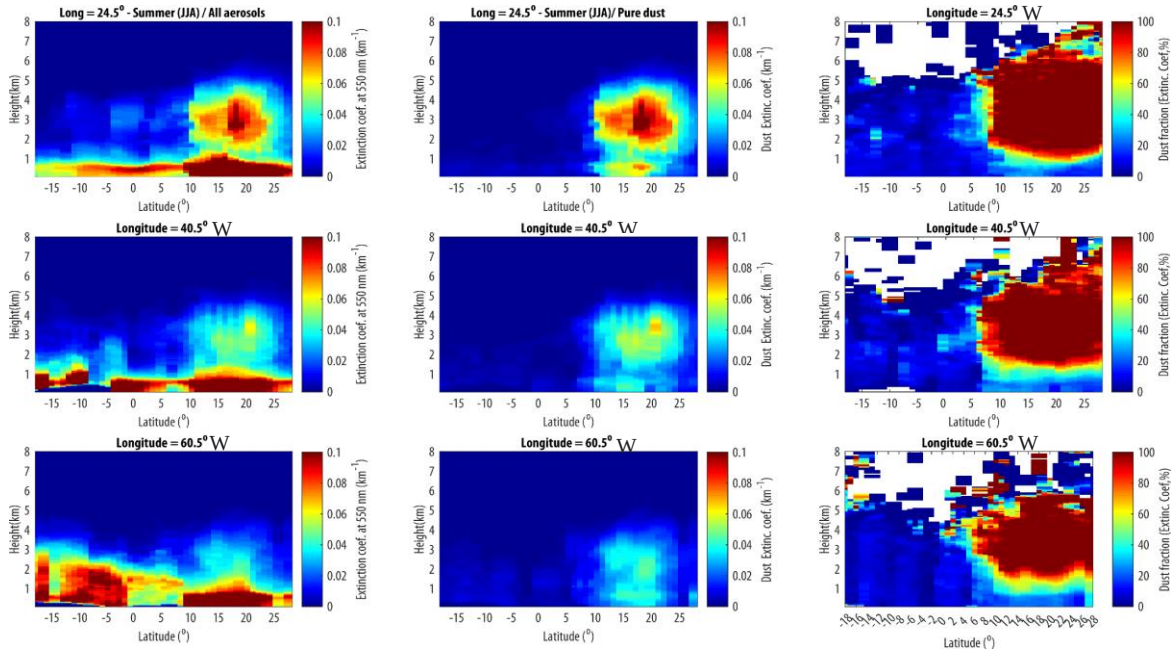

Figure 22: Boreal summer (June - July - August) mean of the latitude-height transect of extinction coefficient (for all aerosols and pure dust) and dust fraction (as a relative contribution to the total extinction coefficient) for three longitudes of reference: Mindelo city (24.5º), Cabo Verde, as a reference to the structure when Saharan dust leave North Africa, elsewhere in the middle of the Atlantic (40.5º) and Manaus city(60.5º), the capital of Amazonia states, in the northern region of South America.

During the autumn season (SON Fig.23), horizontal dust transport patterns show that most of the dust is advected toward the Sahel region and the Gulf of Guinea coastal countries. This

season presents the lowest amount of dust across the source region (DOD < 0.4). However, for all aerosols high AOD values (AOD > 0.6) are identified in the southern portion of West Africa, which is likely to be related to biomass burning aerosols. The high AOD levels also seen in the northeast portion of South America, recognized as mainly related to biomass burning types (Rosario et al., 2013), which are well excluded in LIVAS pure dust products.

As it is possible to see, the dust plume is typically transported to the tropical Atlantic and Americas via the southern part of Cabo Verde. DOD across the southern portion of West Africa indicates values as high as 0.4 decreases to values around 0.2 over the tropical Atlantic and less than 0.1 off the coast of South America.

The extinction coefficient transects (Fig. 24), which indicates the longitudinal transport of dust during autumn from the north of Africa to the tropical Atlantic and Americas, also show the lower amount of dust being transported when compared with the previous analyzed seasons. Another different aspect is that the highest pure dust of extinction coefficient values (0.1 km^{-1}) is observed at the surface for the Mindelo reference longitude, indicating a transport closer to the surface during autumn. With these two aspects, a lower amount of dust leaving North Africa and travelling close to the surface, less aerosol is arriving in the western portion of the tropical Atlantic (Extinction coefficient values < 0.03 km^{-1}). Although dust still contributes to almost 100% of aerosols in the free troposphere, the dust particles at high levels are in much lower quantity during this time.

Moreover, the dust fractions found across Mindelo's reference longitude in the upper levels are smaller than for the summer and spring seasons, varied from 60 to100% between 2 and 5 km), and reaching values lower than 60% from the middle Atlantic to the north coast of South America.

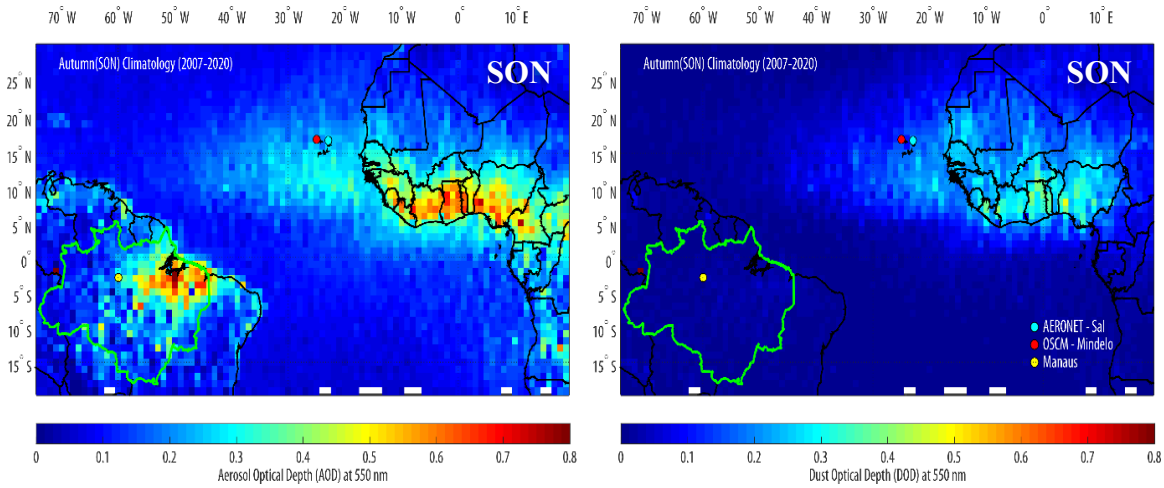

Figure 23: Boreal autumn (September - October - November) climatology of Aerosol Optical Depth (AOD) and Dust Optical Depth (DOD) at 532 nm based on LIVAS aerosol product for the period between 2007 and 2020. The circles markers on the maps indicate the city of Mindelo(red), taken as the reference of the OSCM coordinates, the Sal island (cyan) and Manaus city(yellow), the capital of Amazonia states as a reference for South América.

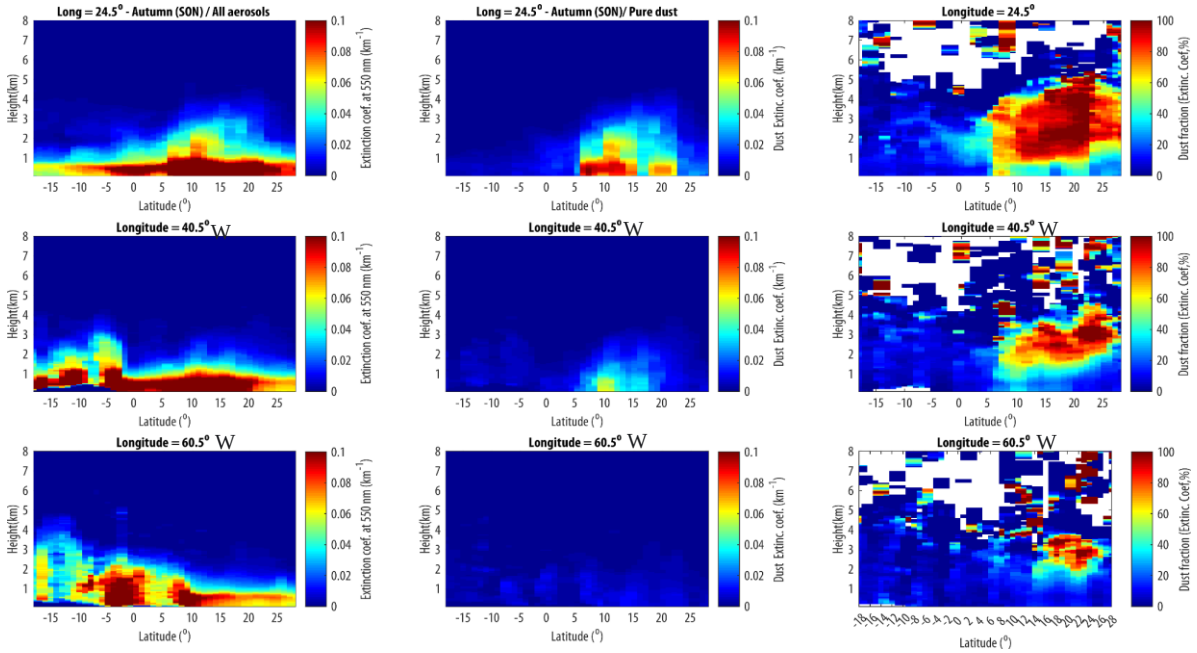

Figure 24: Boreal autumn (September - October - November) mean of the latitude-height transect of extinction coefficient (for all aerosols and pure dust) and dust fraction (as relative contribution to the total extinction coefficient) for three longitude of reference: Mindelo city (24.5º), Cabo Verde, as reference to the structure when Saharan dust leave North Africa, elsewhere in the middle of the Atlantic (40.5º) and Manaus city (60.5º), the capital of Amazonia states, in the northern region of South America.

Figure 25 shows the winter season climatology of AOD and DOD. All aerosols and pure dust plumes' spatial distribution resemble autumn patterns in many aspects, except for the amount of aerosols and dust that are much higher (AOD > 0.7 and DOD > 0.5). As for autumn, different

from the previous season, most of the dust is concentrated in the southern part of North Africa. Therefore, dust transport to the tropical Atlantic occurs typically south of Cabo Verde and moves mainly to the north of South America. The highest values of DOD across North Africa are observed out of the Saharan domain, mostly in the Guinea Gulf countries, which can reveal LIVAS difficulty in achieving full separation of dust from other aerosols, mainly biomass burning types, since Gulf of Guinea countries are strong sources of dust particles. During the dry or winter season, DOD typical values vary from 0.4 to 0.6 over Africa to 0.30 -0.4 in the middle of the tropical Atlantic and decrease to 0.1 - 0.2 over the South American coast. The latitude-altitude transect of the mean extinction coefficient for pure dust and all aerosols, and dust fraction profiles is presented in Figure 26. The extinction coefficients for all aerosols indicate that higher values are observed near the source (Mindelo reference longitude) and at low altitudes. This season dust transport occurs predominantly within MBL, which is an important issue for air quality in Cabo Verde and other countries close to the Sahara. Dust plumes leave North Africa within a broader range of latitude, from less than 5^{o} to almost 25^{o}, but the range is significantly narrowed in the middle of the Atlantic. In the layers from the surface to the free troposphere (up to 3 km), between latitudes of 5^{o} and 10^{o}, a significant amount of aerosol is transported to the middle Atlantic and South America. Dust explains just a fraction of it, less than 70% close to Africa and less than 50% over the middle of the Atlantic. Known from previous studies (Rizzolo *et al*, 2017), during the winter aerosols traveling to South America is a mixture dominated by dust particles and biomass burning aerosols.

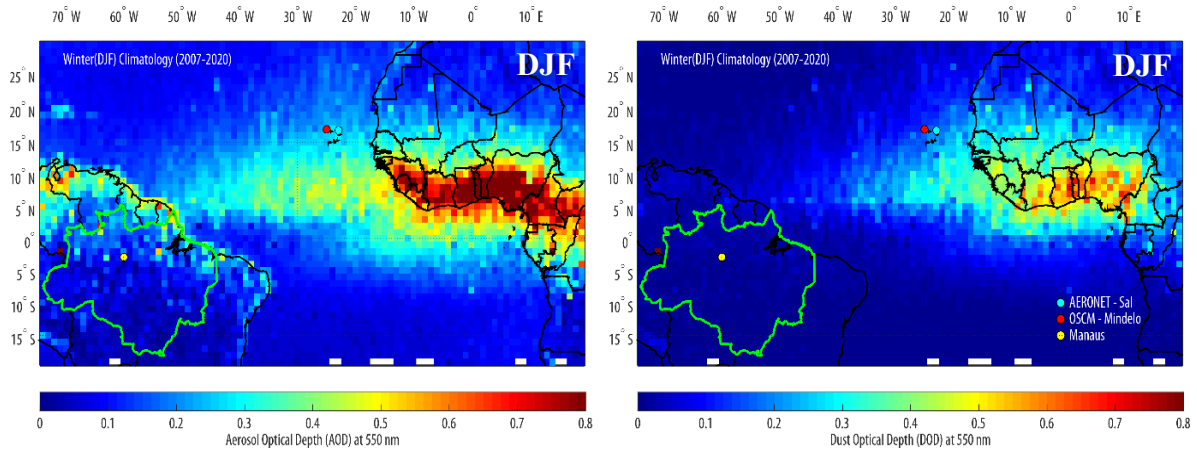

Figure 25: Boreal winter (December - January - February) climatology of Aerosol Optical Depth (AOD) and Dust Optical Depth (DOD) at 532 nm based on LIVAS aerosol product for the period between 2007 and 2020. The circle markers on the maps indicate the city of Mindelo(red), taken as the reference of the OSCM coordinates, the Sal island (cyan) and Manaus city(yellow), the capital of Amazonia states as a reference for South América.

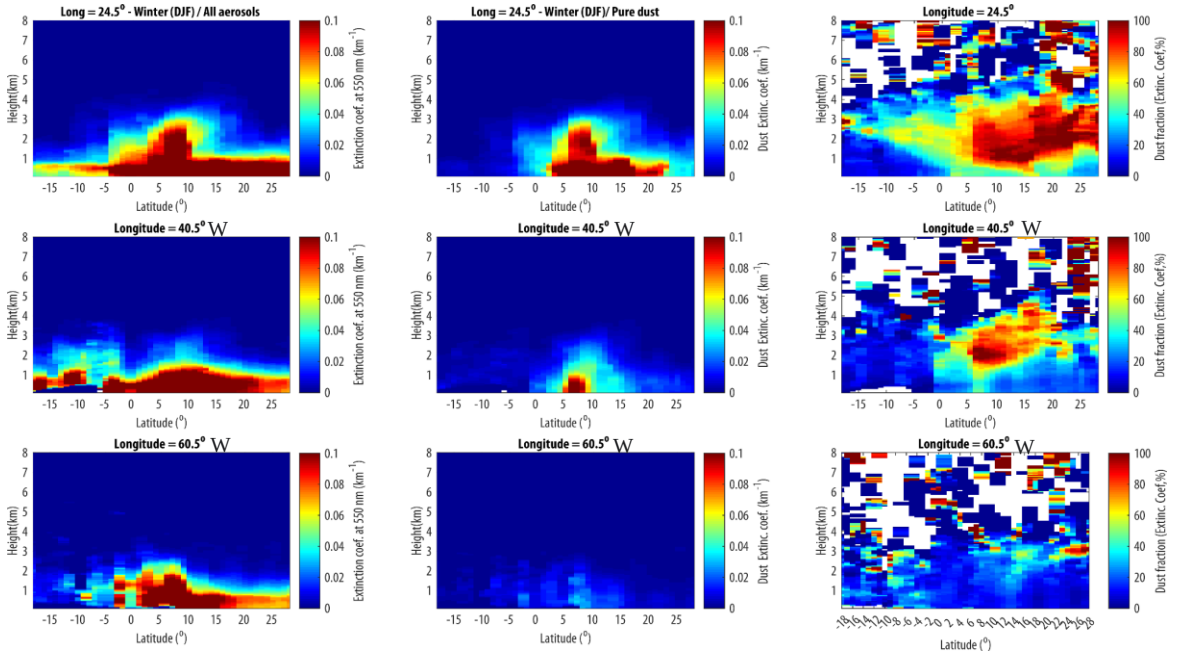

Figure 26: Boreal winter (December - January - February) mean of the latitude-height transect of extinction coefficient (for all aerosols and pure dust), and dust fraction (as a relative contribution to the total extinction coefficient) for three longitudes of reference: Mindelo city (24.5º), Cabo Verde, as a reference to the structure when Saharan dust leave North Africa, elsewhere in the middle of the Atlantic (40.5º) and Manaus city (60.5º), the capital of Amazonia states, in the northern region of South America.

5. Discussion

The present study focused on the evaluation and application of the LIVAS (LIdar climatology of Vertical Aerosol Structure for space-based lidar simulation studies) aerosol product, a 3-D global aerosol optical database (Amiridis *et al*., 2013), to characterize the typical structure of Saharan dust transport over Mindelo City, Cabo Verde and towards remote regions of tropical Atlantic and Americas. Aerosols and dust optical depths (AOD and DOD), alongside profiles of backscattering and extinction coefficients from LIVAS, have been used to perform these tasks. A ground-based LIDAR system (PollyXT, (Baars *et al.*, 2016) operating in Mindelo at OSCM, in Cabo Verde, provided independent backscattering and extinction coefficients profiles to be compared with LIVAS, while independent AOD were taken from AERONET sun photometers operation in Mindelo and Sal island. The current LIVAS global database is based on further processing of CALIPSO Level 2 Cloud and Aerosol Profile Products and its subsequent aggregation on a resolution of 1^{o}x 1^{o}. In this study, it explored the influence of different aggregation radii (100, 200, 300, 400, 500 km).

The intercomparison of the profiles of backscatter and extinction from PollyXT and LIVAS over Mindelo city was initially done for a set of case studies presenting distinct dust transport structures. A good agreement was found in individual case scenarios between backscatter and extinction coefficient measurements with Pollyxt and LIVAS for all, of the tested aggregation radius. A recognized overlap issue for the PollyXT lidar system prevents further comparison between the two products within the Marine Atmospheric Boundary Layer. The comparison results at the monthly scale were even better, revealing an excellent agreement between PollyXT and LIVAS monthly average profiles at all levels, but mainly in the free troposphere, where dust transport is dominant for the period of the comparison. For the smaller aggregation radius (100 and 200 km), non-negligible discrepancies were found at certain levels, which were reduced in the larger radius. This result pointed out that the monthly scale that considered expansion in the aggregation radius, from 100 km to 500 km, did not significantly affect the comparison between LIVAS and Polly. Nevertheless, the increase in the aggregation radius improved LIVAS temporal statistics since, for a specific month the number of profiles for a 100 km radius is substantially lower than for 300 and 500 km. Another relevant aspect is of the PollyXT lidar system, its good agreement with LIVAS at a radius as large as 500 km revealing that at a monthly scale, PollyXT presents an extended regional representativity (Mielonen *et al*., 2000).

Also found good agreement between CALIPSO and PollyXT backscatter and extinction profiles over India and South African cities. The maximum distances between the CALIPSO overpasses and the reference sites in their study range from 50 km to about 100 km. The main reason for the difference that they found was the distance between the CALIPSO track and the measurement sites since the distance enables differences in air masses and cloudiness.

After the comparison between LIVAS and Polly, LIVAS products (AOD, DOD, and extinction and backscatter profiles) were used to characterize the annual cycle and the vertical structure of aerosols and pure dust over Mindelo. From January to April, there are fewer aerosols over Mindelo City and over Cabo Verde in general. On average, LIVAS AOD varies from values below 0.2 to 0.3. The largest AOD means and variability is found from May to October, with a peak in June and July between 0.5 to 0.7, and then a decrease to values around 0.2 from November to December is observed. These monthly mean variabilities are consistent with AERONET long-term station in Cabo Verde, at Sal Island, and with results from previous studies. Holben et al. (2001) found AOD at 500 nm to vary from 0.26 in April to approximately 0.7 in June. For lower aerosol periods (January to April) LIVAS tends to present lower monthly mean AOD when compared with AERONET. (Omar *et al*., 2013) also show that CALIPSO AOD tends to be lower than AERONET AOD at low optical depths. Among potential sources of error associated with environmental conditions, they pointed out cloud contamination and scene inhomogeneity. Pure dust optical depth (DOD) shows a similar mean annual cycle, increasing during the summer and decreasing during winter. Values varied from ~0.1 (January) to ~0.35 (June) for the larger radius (500 km), which shows the highest DOD values among the radii.

These results corroborate previous analysis that dust is the main driver of AOD seasonality in Cabo Verde. The seasonal variability in the vertical distribution of dust can be broadly understood in the context of the ITCZ and West Africa Monsoon seasonal dynamic. During the onset of monsoon MAM in the region, ITCZ moves progressively northward. Consequently, dust particles are averted in higher layers compared to the months of DJF. However, during the JJA season, WAM is fully developed over land, and dust particles are lifted into upper levels of the atmosphere. While in SON, dust concentration in the upper layers of the atmosphere is reduced due to the retreat of the ITD from the region. Therefore, the convergence of harmattan and monsoon surface winds along the ITD frontal zone contributes to dust particle lift in the upper layers of the atmosphere during the summer (Tulet *et al*., 2008).

Regarding the radius dependence, we did not see significant differences for AOD climatology. However, for DOD there is a clear dependence with smaller radii presenting lower mean DOD. In addition, important differences were observed among the radii for monthly interannual variability, mainly for the 100 km. From year to year (2006 to 2021), the seasonal cycle, in both AOD and DOD, is less structured for the smallest radii (100, 200 km). Two aspects can contribute to this: a) for the smallest radii (100 and 200 km) statistics, are less robust since the profile number per month is much lower; b) and smaller radius sample limited domain, therefore its odds of capturing a higher number of dust transport events is lower.

It is worth emphasizing that the seasonal cycles of AOD and DOD are opposite to the seasonality of aerosol concentrations at the surface level in Cabo Verde. According to (Gama *et al*., 2015), aerosol particles mean monthly concentration at the surface have peaks during the winter season in Cabo Verde, while AOD and DOD peak in summer. During the peak of DOD and AOD, between June and September, most of the particles are transported aloft of the MBL in the free troposphere, with lower influence at the surface levels.

The seasonal variability of the backscatter and extinction coefficient profiles shows that most of the dust transported over Mindelo has its maximum between 2 to 5 km and occurs from June to September. Meanwhile, during the winter season, from December to January, aerosol loading in the free troposphere is dramatically reduced. During this period most of the dust is transported within the marine layer in the shallowest layer, up to 1.5 - 3 km (Barreto *et al*., 2022), and aerosols are concentrated in the MLB. These results are also consistent with (Gama *et al*., 2015), which show that during the winter season, the transport of Saharan dust occurs at near-surface layers, while in the summer, the dust layer is extended to higher levels (up to 5km) over Cape Verde. The dust sources in the Sahel are mostly active during winter and spring, while those located in northern subtropical Saharan latitudes are more active during spring and summer (Prospero *et al*., 2020). All aggregation radii presented similar mean vertical structures of aerosols and dust over Mindelo, except for the magnitude of the extinction and backscatter at certain levels. For instance, from August to October, there is a peak in extinction for all aerosols at the surface for a radius of 100 km, which gets diluted as the radius increases.

It is evident that at this level, aerosols are a mixing of dust with other aerosol types since pure dust alone does not explain this peak at the surface. The mean contribution of dust to the backscatter and extinction of aerosol varies along the altitude and from season to season. Summer presented the highest contribution in the free troposphere, explaining almost 100% of

the extinction and backscatter, followed by spring and autumn. For these three seasons dust relative contribution is quite stable from 1.5 km to 5.0 km. For the MBL dust contribution decreases to lower than 25%. For the winter dust contribution has a distinct behavior, it decreases from values above 50% at 1.5 km to values lower than 25% above 5 km. Meanwhile, in the MBL, dust fraction decreases from 50% at around 1 km to a value lower than 25% close to the surface (Gama *et al*., 2015) found a yearly contribution of 42% of dust from North African deserts for PM10 levels observed in Cape Verde.

Finally, the annual and seasonal cycle of horizontal distribution of aerosols and pure dust (AOD, DOD) and their vertical structure (based on the extinction coefficient profile) were used to characterize the typical transport of Saharan dust to tropical Atlantic and Americas. The dust transport structure displays important meridional displacement and magnitude from season to season. Most of the dust is transported during spring and summer. However, while during the spring season the transport is confined to areas close to the equator (5^o to 15^o), during the summer the dust transport is displaced northward from 10^o to 25^o, as response to the ITCZ northward movement (Yu et al., 2019). During this season, most of the dust is transported to the Caribbean, Central America and south of North America (Prospero, 1972; Omar *et al*., 2013). The transport takes place mostly between the altitude of 2 and 4 km. The autumn season is when the lowest amount of dust is transported toward the Americas, most of it transported in the MBL. That is also the case for winter when the dust layer is transported toward the South America direction and is situated within the lowest 2 km of the troposphere. These results are consistent with the previous studies (Chiapello & Moulin *et al*., 2002; Schepanski *et al*., 2009). Winter is the season that presents the highest decay in the amount of aerosol between the eastern tropical Atlantic and the western portion, with results consistent with (Yu *et al*., 2019) results.

6. Conclusions

This thesis sought to study dust aerosol transport from North Africa, over the Eastern tropical Atlantic (Cabo Verde) and towards remote regions of the Americas using the recently developed product LIVAS, a 3-D multi-wavelength aerosol/cloud database based on CALIPSO (Cloud-Aerosol Lidar and Infrared Pathfinder Satellite Observation) and EARLINET(Amiridis *et al*., 2015). The LIVAS database provides averaged profiles of aerosol optical properties for wavelengths of 355, 532, 1064, 1570, and 2050 nm and of cloud optical properties at 532 nm. It is a valuable database for aerosol meteorological and climatological observational studies and model evaluation. Therefore, an exhaustive evaluation and application of the LIVAS products is imperative.

Cabo Verde islands are in a unique position to study Saharan dust plumes as they leave the continent, their interaction with other atmospheric processes, and their mixture with marine and other aerosol types**.** Additionally, due to a set of advanced ground-based instrumentations being operated at Mindelo city, in São Vicente Island, Cabo Verde has been a hotspot site for remote sensing and models aerosol products evaluation. The first step of this work was to perform a comparison, for a set of study cases, between LIVAS aerosols extinction and backscatter coefficient profiles and a PollyXT Lidar System that has been operated at Mindelo city. Despite the distance between CALIPSO overpass and PollyXT location and the regional atmosphere inhomogeneity, the results show that LIVAS and Pollyxt, have a good agreement in describing distinct scenarios of aerosol and dust transport over Cabo Verde, regardless the aggregation radius adopted (100, 200, 300, 400, 500 km) to applied to CALIPSO profiles in order to set LIVAS product resolutions. The comparison at monthly scale, taken average of September 2021 as a reference, revealed an even better agreement between LIVAS and PollyXT profiles, specially for the free troposphere, where dust is the dominant aerosol. This result LIVAS product quality in describing Saharan dust structure in the eastern tropical Atlantic and to evaluate PollyXT product spatial representativity.

The annual cycle and inter-annual analysis of AOD over Mindelo based on LIVAS revealed that AOD over the radii center at the city occurs from May to October, consistent with previous studies and with AERONET climatology. Similar results were found for DOD, showing that dust is the main driver of aerosols columnar optical properties seasonality over the Cabo Verde region. The seasonality pattern was better defined for larger radii (300, 400, 500 km) than for smaller radii (100 and 200 km). A larger sampling domain and higher number of profiles for

radii 300, 400, and 500 km against reduced domain and profile numbers could explain the difference between the seasonal cycle features of AOD and DOD among the radii. Despite this difference, climatological seasonal cycles for AOD do feature significant differences among the radii. This was not the case for DOD, which presented a dependence with radius, with a larger radius (300, 400, 500 km) characterized by larger AOD when compared with 200 and 100 km radii. For the mean seasonal cycle of vertical profile of backscatter and extinction coefficients over Cabo Verde, LIVAS produced the well-established structure for the seasonal transport of Saharan dust, characterized by low-level transport of dust during the boreal winter and a prevalence of transport during the summer in the free troposphere with a peak between 2 and 5 km. For summer, dust aerosols respond to almost 90% of the aerosol backscatter from 2 to 6 km, while in MBL the relative contribution decreases to less than 25%. During the winter, dust contribution to backscatter in most of the free troposphere is lower than 50%, according to LIVAS. The relative contribution of dust to extinction and backscatter did not present a relevant dependency on radius.

LIVAS application to describe the seasonal transport of Saharan dust to remote western areas of tropical Atlantic and Americas also depicted the patterns consistent with the previous studies on Saharan dust transatlantic transport. The magnitudes of dust transport, as identified by the extinction coefficient profile, are highest in boreal summer and spring and lowest in autumn. The meridional northward shifts of the dust plume is larger during the summer, reaching the latitude of 25^{o}. This summer further displacement are mainly modulated by the seasonal migration of the intertropical convergence zone (ITCZ), and it leads to strong transport of dust toward Central America and the Caribbean.

Winter is the season that the lowest amount of dust is arriving in the remote western Atlantic. This can be explained by the low-latitude transport of dust and probably an efficiency loss of dust particles along the way due to the ITCZ interception. Additionally, winter season is when most Saharan dust transport is towards South America, and more specifically toward the Amazon basin, a feature captured by the LIVAS dataset.

LIVAS 3D aerosol optical properties provide a relevant database for aerosol study from regional to global scales and from meteorological perspective to climatological analysis. We were able to characterize the seasonal cycle of aerosol vertical structure over a specific place, Mindelo City, Cabo Verde, and across a vast area of the tropical Atlantic. LIVAS spatial mean optical properties seem to have a certain dependency on the aggregation radius, at least for monthly time scale, and especially for the columnar optical properties. A smaller aggregation

radius (< 200 km) limits the number of profiles and, therefore, may affect the statistics. This can be relevant to studies that focused on the interannual variability of dust transport, an aspect that was not comprehensively analyzed in this study. Another aspect that was not further explored is the effect of inhomogeneity of the atmosphere in the comparison between LIVAS and PollyXT. These can be pointed out some of the limitations of the present study.

7. Recommendations

- More research is needed to understand the difference between PollyXT and LIVAS around Mindelo and better explore the role of atmosphere inhomogeneity, CALIPSO overpass distance and possible cloud contamination.
- This study focused mainly on the climatological structure of aerosols and dust articles over Cabo Verde and during their transport towards remote areas of the Atlantic. Therefore, there is a need to explore and evaluate LIVAS aerosol products ability to describe the interannual variability of aerosol and dust structure across the Atlantic tropical basin.

8. References

Amiridis, V., Marinou, E., Tsekeri, A., Wandinger, U., Schwarz, A., Giannakaki, E., Mamouri, R., Kokkalis, P., Binietoglou, I., Solomos, S., Herekakis, T., Kazadzis, S., Gerasopoulos, E., Balis, D., Papayannis, A., Kontoes, C., Kourtidis, K., Papagiannopoulos, N., Mona, L., … Ansmann, A. (2015). LIVAS: a 3-D multi-wavelength aerosol/cloud climatology LIVAS: a 3-D multi-wavelength aerosol/cloud climatology based on CALIPSO and EARLINET LIVAS: a 3-D multi-wavelength aerosol/cloud climatology. *Atmos. Chem. Phys. Discuss*, *15*(March), 2247–2304. https://doi.org/10.5194/acpd-15-2247-2015

Amiridis, V., Wandinger, U., Marinou, E., Giannakaki, E., Tsekeri, A., Basart, S., Kazadzis, S., Gkikas, A., Taylor, M., Baldasano, J., & Ansmann, A. (2013). Optimizing CALIPSO saharan dust retrievals. *Atmospheric Chemistry and Physics*, *13*(23), 12089–12106. https://doi.org/10.5194/acp-13-12089-2013

Amiridis, V., Wandinger, U., Marinou, E., & Tsekeri, A. (2014). *LIVAS*.

Ansmann, A., Bösenberg, J., Chiakovsky, A., Comerón, A., Eckhardt, S., Eixmann, R., Freudenthaler, V., Ginoux, P., Komguem, L., Linné, H., Lopez Marquez, M. Á., Matthias, V., Mattis, I., Mitev, V., Müller, D., Music, S., Nickovic, S., Pelon, J., Sauvage, L., … Wiegner, M. (2003). Long-range transport of Saharan dust to northern Europe: The 11-16 October 2001 outbreak observed with EARLINET. *Journal of Geophysical Research: Atmospheres*, *108*(24), 1–15. https://doi.org/10.1029/2003jd003757

Ansmann, A., Petzold, A., Kandler, K., Tegen, I., Wendisch, M., Müller, D., Weinzierl, B., Müller, T., & Heintzenberg, J. (2011). Saharan Mineral Dust Experiments SAMUM-1 and SAMUM-2: What have we learned? *Tellus, Series B: Chemical and Physical Meteorology*, *63*(4), 403–429. https://doi.org/10.1111/j.1600-0889.2011.00555.x

Ansmann, A., Riebesell, M., & Weitkamp, C. (1990). Measurement of atmospheric aerosol extinction profiles with a Raman lidar. *Optics Letters*, *15*(13), 746. https://doi.org/10.1364/ol.15.000746

Baars, H., Kanitz, T., Engelmann, R., Althausen, D., Heese, B., Komppula, M., Preißler, J., Tesche, M., Ansmann, A., Wandinger, U., Lim, J. H., Young Ahn, J., Stachlewska, I. S., Amiridis, V., Marinou, E., Seifert, P., Hofer, J., Skupin, A., Schneider, F., … Zamorano, F. (2016). An overview of the first decade of PollyNET: An emerging network of automated Raman-polarization lidars for continuous aerosol profiling. *Atmospheric Chemistry and Physics*, *16*(8), 5111–5137. https://doi.org/10.5194/acp-16-5111-2016

Balkanski, Y., Schulz, M., Claquin, T., & Guibert, S. (2007). Reevaluation of Mineral aerosol radiative forcings suggests a better agreement with satellite and AERONET data. *Atmospheric Chemistry and Physics*, *7*(1), 81–95. https://doi.org/10.5194/acp-7-81-2007

Barkley, A. E., Pourmand, A., Longman, J., Sharifi, A., Prospero, J. M., Panechou, K., Bakker, N., Drake, N., Guinoiseau, D., & Gaston, C. J. (2022). Interannual Variability in the Source Location of North African Dust Transported to the Amazon. *Geophysical Research Letters*, *49*(10), 1–11. https://doi.org/10.1029/2021GL097344

Barreto, Á., Cuevas, E., Garciá, R. D., Carrillo, J., Prospero, J. M., Ilić, L., Basart, S., Berjón, A. J., Marrero, C. L., Hernández, Y., Bustos, J. J., Ničković, S., & Yela, M. (2022). Long-term characterisation of the vertical structure of the Saharan Air Layer over the Canary Islands using lidar and radiosonde profiles: Implications for radiative and cloud processes over the subtropical Atlantic Ocean. *Atmospheric Chemistry and Physics*, *22*(2), 739–763. https://doi.org/10.5194/acp-22-739-2022

Ben-Ami, Y., Koren, I., Altaratz, O., Kostinski, A., & Lehahn, Y. (2012). Discernible rhythm in the spatio/temporal distributions of transatlantic dust. *Atmospheric Chemistry and Physics*, *12*(5), 2253–2262. https://doi.org/10.5194/acp-12-2253-2012

Biele, J., Beyerle, G., & Baumgarten, G. (2000). Polarization Lidar: Correction of instrumental effects. *Optics Express*, *7*(12), 427. https://doi.org/10.1364/oe.7.000427

Chiapello, I., & Moulin, C. (2002). TOMS and METEOSAT satellite records of the variability of Saharan dust transport over the Atlantic during the last two decades (1979-1997). *Geophysical Research Letters*, *29*(8), 2–5. https://doi.org/10.1029/2001GL013767

DeMott, P. J., Sassen, K., Poellot, M. R., Baumgardner, D., Rogers, D. C., Brooks, S. D., Prenni, A. J., & Kreidenweis, S. M. (2003). African dust aerosols as atmospheric ice nuclei. *Geophysical Research Letters*, *30*(14), 26–29. https://doi.org/10.1029/2003GL017410

Di, L., Yu, E. G., Yang, Z., Shrestha, R., Kang, L., Zhang, B., & Sw, I. A. (2015). *REMOTE SENSING BASED CROP GROWTH STAGE ESTIMATION MODEL 1 . Center for Spatial Information Science and Systems , George Mason University , 4400 University Drive , MSN 6E1 , Fairfax , VA 22030 , USA 2 . National Agricultural Statistics Service , United Sta*. 2739–2742.

Doherty, O. M., Riemer, N., & Hameed, S. (2014). Role of the convergence zone over West Africa in controlling Saharan mineral dust load and transport in the boreal summer. *Tellus, Series B: Chemical and Physical Meteorology*, *66*(1), 1–19. https://doi.org/10.3402/tellusb.v66.23191

Dunion, J. P., & Velden, C. S. (2004). The impact of the Saharan Air Layer on Atlantic tropical cyclone activity. *Bulletin of the American Meteorological Society*, *85*(3), 353–365. https://doi.org/10.1175/BAMS-85-3-353

Evan, A. T., & Mukhopadhyay, S. (2010). African dust over the northern tropical Atlantic: 1955-2008. *Journal of Applied Meteorology and Climatology*, *49*(11), 2213–2229. https://doi.org/10.1175/2010JAMC2485.1

Gama, C., Tchepel, O., Baldasano, J. M., Basart, S., Ferreira, J., Pio, C., Cardoso, J., & Borrego, C. (2015). Seasonal patterns of Saharan dust over Cape Verde - a combined approach using observations and modelling. *Tellus, Series B: Chemical and Physical Meteorology*, *67*(1), 1–21. https://doi.org/10.3402/tellusb.v67.24410

Georgoulias, A. K., Tsikerdekis, A., Amiridis, V., Marinou, E., Benedetti, A., Zanis, P., Alexandri, G., Mona, L., Kourtidis, K. A., & Lelieveld, J. (2018). A 3-D evaluation of the MACC reanalysis dust product over Europe, northern Africa and Middle East using CALIOP/CALIPSO dust satellite observations. *Atmospheric Chemistry and Physics*, *18*(12), 8601–8620. https://doi.org/10.5194/acp-18-8601-2018

Gläser, G., Wernli, H., Kerkweg, A., & Teubler, F. (2015). The transatlantic dust transport from North Africa to the Americas—its characteristics and source regions. *Journal of Geophysical Research*, *120*(21), 11,231-11,252. https://doi.org/10.1002/2015JD023792

Holben, B. N., Eck, T. F., Slutsker, I., Tanré, D., Buis, J. P., Setzer, A., Vermote, E., Reagan, J. A., Kaufman, Y. J., Nakajima, T., Lavenu, F., Jankowiak, I., & Smirnov, A. (1998). AERONET - A federated instrument network and data archive for aerosol characterization. *Remote Sensing of Environment*, *66*(1), 1–16. https://doi.org/10.1016/S0034-4257(98)00031-5

Huneeus, N., Schulz, M., Balkanski, Y., Griesfeller, J., Prospero, J., Kinne, S., Bauer, S.,

Boucher, O., Chin, M., Dentener, F., Diehl, T., Easter, R., Fillmore, D., Ghan, S., Ginoux, P., Grini, A., Horowitz, L., Koch, D., Krol, M. C., … Zender, C. S. (2011). Global dust model intercomparison in AeroCom phase i. *Atmospheric Chemistry and Physics*, *11*(15), 7781–7816. https://doi.org/10.5194/acp-11-7781-2011

Israelevich, P. L., Ganor, E., Levin, Z., & Joseph, J. H. (2003). Annual variations of physical properties of desert dust over Israel. *Journal of Geophysical Research: Atmospheres*, *108*(13), 1–9. https://doi.org/10.1029/2002jd003163

Jickells, T. D., An, Z. S., Andersen, K. K., Baker, A. R., Bergametti, C., Brooks, N., Cao, J. J., Boyd, P. W., Duce, R. A., Hunter, K. A., Kawahata, H., Kubilay, N., LaRoche, J., Liss, P. S., Mahowald, N., Prospero, J. M., Ridgwell, A. J., Tegen, I., & Torres, R. (2005). Global iron connections between desert dust, ocean biogeochemistry, and climate. *Science*, *308*(5718), 67–71. https://doi.org/10.1126/science.1105959

Kaufman, Y. J., Koren, I., Remer, L. A., Rosenfeld, D., & Rudich, Y. (2005). The effect of smoke, dust, and pollution aerosol on shallow cloud development over the Atlantic Ocean. *Proceedings of the National Academy of Sciences of the United States of America*, *102*(32), 11207–11212. https://doi.org/10.1073/pnas.0505191102

Kaufman, Y. J., Tanré, D., & Boucher, O. (2002). A satellite view of aerosols in the climate system. *Nature*, *419*(6903), 215–223. https://doi.org/10.1038/nature01091

Kishcha, P., Barnaba, F., Gobbi, G. P., Alpert, P., Shtivelman, A., Krichak, S. O., & Joseph, J. H. (2005). Vertical distribution of Saharan dust over Rome (Italy): Comparison between 3-year model predictions and lidar soundings. *Journal of Geophysical Research D: Atmospheres*, *110*(6), 1–16. https://doi.org/10.1029/2004JD005480

Knippertz, P., & Stuut, J. B. W. (2014). Mineral dust: A key player in the earth system. *Mineral Dust: A Key Player in the Earth System*, 1–509. https://doi.org/10.1007/978-94-017-8978-3

Kok, J. F., Adebiyi, A. A., Albani, S., Balkanski, Y., Checa-Garcia, R., Chin, M., Colarco, P. R., Hamilton, D. S., Huang, Y., Ito, A., Klose, M., Li, L., Mahowald, N. M., Miller, R. L., Obiso, V., Pérez García-Pando, C., Rocha-Lima, A., & Wan, J. S. (2021). Contribution of the world's main dust source regions to the global cycle of desert dust. *Atmospheric Chemistry and Physics*, *21*(10), 8169–8193. https://doi.org/10.5194/acp-21-8169-2021

Koren, I., Remer, L. A., Altaratz, O., Martins, J. V., & Davidi, A. (2010). Aerosol-induced changes of convective cloud anvils produce strong climate warming. *Atmospheric Chemistry and Physics*, *10*(10), 5001–5010. https://doi.org/10.5194/acp-10-5001-2010

Mahowald, N., Jickells, T. D., Baker, A. R., Artaxo, P., Benitez-Nelson, C. R., Bergametti, G., Bond, T. C., Chen, Y., Cohen, D. D., Herut, B., Kubilay, N., Losno, R., Luo, C., Maenhaut, W., McGee, K. A., Okin, G. S., Siefert, R. L., & Tsukuda, S. (2008). Global distribution of atmospheric phosphorus sources, concentrations and deposition rates, and anthropogenic impacts. *Global Biogeochemical Cycles*, *22*(4), 1–19. https://doi.org/10.1029/2008GB003240

Mahowald, N. M., Baker, A. R., Bergametti, G., Brooks, N., Duce, R. A., Jickells, T. D., Kubilay, N., Prospero, J. M., & Tegen, I. (2005). Atmospheric global dust cycle and iron inputs to the ocean. *Global Biogeochemical Cycles*, *19*(4). https://doi.org/10.1029/2004GB002402

Mamouri, R. E., & Ansmann, A. (2016). Potential of polarization lidar to provide profiles of CCN-and INP-relevant aerosol parameters. *Atmospheric Chemistry and Physics*, *16*(9),

5905–5931. https://doi.org/10.5194/acp-16-5905-2016

Marinou, E., Amiridis, V., Binietoglou, I., Tsikerdekis, A., Solomos, S., Proestakis, E., Konsta, Di., Papagiannopoulos, N., Tsekeri, A., Vlastou, G., Zanis, P., Balis, Di., Wandinger, U., & Ansmann, A. (2017). Three-dimensional evolution of Saharan dust transport towards Europe based on a 9-year EARLINET-optimized CALIPSO dataset. *Atmospheric Chemistry and Physics*, *17*(9), 5893–5919. https://doi.org/10.5194/acp-17-5893-2017

Marinou, E., Amiridis, V., Paschou, P., Tsikoudi, I., Tsekeri, A., Daskalopoulou, V., Baars, H., Floutsi, A., Kouklaki, D., & Pirloaga, R. (2023). ASKOS Campaign 2021/2022: Overview of measurements and applications. *EGU23*, *EGU23-16530*.

Meskhidze, N., Chameides, W. L., & Nenes, A. (2005). Dust and pollution: A recipe for enhanced ocean fertilization? *Journal of Geophysical Research D: Atmospheres*, *110*(3), 1–23. https://doi.org/10.1029/2004JD005082

Mielonen, T., Giannakaki, E., Omar, A., Arola, A., Lehtinen, K. E. J., Komppula, M., & Unit, K. (2000). *Evaluation of Caliop Level 2 Aerosol Profiles With Ground-Based Lidar Measurements in India and South Africa*. *1*, 2–5.

Moran-Zuloaga, D., Ditas, F., Walter, D., Saturno, J., Brito, J., Carbone, S., Chi, X., Hrabě De Angelis, I., Baars, H., H M Godoi, R., Heese, B., A Holanda, B., Lavrič, J. V., Martin, S., Ming, J., L Pöhlker, M., Ruckteschler, N., Su, H., Wang, Y., … Pöhlker, C. (2018). Long-term study on coarse mode aerosols in the Amazon rain forest with the frequent intrusion of Saharan dust plumes. *Atmospheric Chemistry and Physics*, *18*(13), 10055–10088. https://doi.org/10.5194/acp-18-10055-2018

Moulin, C., Lambert, C. E., Dayan, U., Masson, V., Ramonet, M., Bousquet, P., Legrand, M., Balkanski, Y. J., Guelle, W., Marticorena, B., Bergametti, G., & Dulac, F. (1998). Satellite climatology of African dust transport in the Mediterranean atmosphere. *Journal of Geophysical Research Atmospheres*, *103*(D11), 13137–13144. https://doi.org/10.1029/98JD00171

Muhs, D. R., Budahn, J. R., Prospero, J. M., & Carey, S. N. (2007). Geochemical evidence for African dust inputs to soils of western Atlantic islands: Barbados, the Bahamas, and Florida. *Journal of Geophysical Research: Earth Surface*, *112*(2), 1–26. https://doi.org/10.1029/2005JF000445

Omar, A. H., Winker, D. M., Kittaka, C., Vaughan, M. A., Liu, Z., Hu, Y., Trepte, C. R., Rogers, R. R., Ferrare, R. A., Lee, K. P., Kuehn, R. E., & Hostetler, C. A. (2009). The CALIPSO automated aerosol classification and lidar ratio selection algorithm. *Journal of Atmospheric and Oceanic Technology*, *26*(10), 1994–2014. https://doi.org/10.1175/2009JTECHA1231.1

Omar, A. H., Winker, D. M., Tackett, J. L., Giles, D. M., Kar, J., Liu, Z., Vaughan, M. A., Powell, K. A., & Trepte, C. R. (2013). CALIOP and AERONET aerosol optical depth comparisons: One size fits none. *Journal of Geophysical Research Atmospheres*, *118*(10), 4748–4766. https://doi.org/10.1002/jgrd.50330

Papayannis, A., Amiridis, V., Mona, L., Tsaknakis, G., Balis, D., Bösenberg, J., Chaikovski, A., De Tomasi, F., Grigorov, I., Mattis, I., Mitev, V., Müller, D., Nickovic, S., Pérez, C., Pietruczuk, A., Pisani, G., Ravetta, F., Rizi, V., Sicard, M., … Pappalardo, G. (2008). Systematic lidar observations of Saharan dust over Europe in the frame of EARLINET (2000-2002). *Journal of Geophysical Research Atmospheres*, *113*(10), 1–17. https://doi.org/10.1029/2007JD009028

Pappalardo, G., Amodeo, A., Apituley, A., Comeron, A., Freudenthaler, V., Linné, H., Ansmann, A., Bösenberg, J., D'Amico, G., Mattis, I., Mona, L., Wandinger, U., Amiridis, V., Alados-Arboledas, L., Nicolae, D., & Wiegner, M. (2014). EARLINET: Towards an advanced sustainable European aerosol lidar network. *Atmospheric Measurement Techniques*, *7*(8), 2389–2409. https://doi.org/10.5194/amt-7-2389-2014

Prospero, J. M. (1972). *Vertical and Areal Distribution of Saharan Dust over the Western During the Barbados Oceanographic air below . In this paper , we present by first extracting*. *77*(27), 5255–5265.

Prospero, J. M. (1996). *Saharan Dust Transport Over the North Atlantic Ocean and Mediterranean: An Overview*. 133–151. https://doi.org/10.1007/978-94-017-3354-0_13

Prospero, J. M., Barkley, A. E., Gaston, C. J., Gatineau, A., Campos y Sansano, A., & Panechou, K. (2020). Characterizing and Quantifying African Dust Transport and Deposition to South America: Implications for the Phosphorus Budget in the Amazon Basin. *Global Biogeochemical Cycles*, *34*(9), 1–24. https://doi.org/10.1029/2020GB006536

Prospero, J. M., & Carlson, T. N. (1980). Saharan air outbreaks over the tropical North Atlantic. *Pure and Applied Geophysics PAGEOPH*, *119*(3), 677–691. https://doi.org/10.1007/BF00878167

Prospero, J. M., Glaccum, R. A., & Nees, R. T. (1981). Atmospheric transport of soil dust from Africa to South America. *Nature*, *289*(5798), 570–572. https://doi.org/10.1038/289570a0

Prospero, J. M., & Lamb, P. J. (2003). African Droughts and Dust Transport to the Caribbean: Climate Change Implications. *Science*, *302*(5647), 1024–1027. https://doi.org/10.1126/science.1089915

Prospero, J. M., & Mayol-Bracero, O. L. (2013). Understanding the transport and impact of African dust on the Caribbean Basin. *Bulletin of the American Meteorological Society*, *94*(9), 1329–1337. https://doi.org/10.1175/BAMS-D-12-00142.1

Ramanathan, V., Crutzen, P. J., Kiehl, J. T., & Rosenfeld, D. (2001). Aerosols, Climate, and the Hydrological Cycle. *New Series*, *294*(5549), 2119–2124. https://www.jstor.org/stable/pdf/3085348.pdf?refreqid=excelsior%3A2e030721449f51ab196555d18edb1ba1

Randles, C. A., da Silva, A. M., Buchard, V., Colarco, P. R., Darmenov, A., Govindaraju, R., Smirnov, A., Holben, B., Ferrare, R., Hair, J., Shinozuka, Y., & Flynn, C. J. (2017). The MERRA-2 aerosol reanalysis, 1980 onward. Part I: System description and data assimilation evaluation. *Journal of Climate*, *30*(17), 6823–6850. https://doi.org/10.1175/JCLI-D-16-0609.1

Ridame, C., Dekaezemacker, J., Guieu, C., Bonnet, S., L'Helguen, S., & Malien, F. (2014). Contrasted Saharan dust events in LNLC environments: Impact on nutrient dynamics and primary production. *Biogeosciences*, *11*(17), 4783–4800. https://doi.org/10.5194/bg-11-4783-2014

Rizzolo, J. A., Barbosa, C. G. G., Borillo, G. C., Godoi, A. F. L., Souza, R. A. F., Andreoli, R. V., Manzi, A. O., Sá, M. O., Alves, E. G., Pöhlker, C., Angelis, I. H., Ditas, F., Saturno, J., Moran-Zuloaga, D., Rizzo, L. V., Rosário, N. E., Pauliquevis, T., Santos, R. M. N., Yamamoto, C. I., … Godoi, R. H. M. (2017). Soluble iron nutrients in Saharan dust over the central Amazon rainforest. *Atmospheric Chemistry and Physics*, *17*(4), 2673–2687. https://doi.org/10.5194/acp-17-2673-2017

Ryder, C. L., Marenco, F., Brooke, J. K., Estelles, V., Cotton, R., Formenti, P., McQuaid, J. B., Price, H. C., Liu, D., Ausset, P., Rosenberg, P. D., Taylor, J. W., Choularton, T., Bower, K., Coe, H., Gallagher, M., Crosier, J., Lloyd, G., Highwood, E. J., & Murray, B. J. (2018). Coarse-mode mineral dust size distributions, composition and optical properties from AER-D aircraft measurements over the tropical eastern Atlantic. *Atmospheric Chemistry and Physics*, *18*(23), 17225–17257. https://doi.org/10.5194/acp-18-17225-2018

Schepanski, K., Tegen, I., & Macke, A. (2012). Comparison of satellite based observations of Saharan dust source areas. *Remote Sensing of Environment*, *123*, 90–97. https://doi.org/10.1016/j.rse.2012.03.019

Schepanski, K., Tegen, I., & MacKe, A. (2009). Saharan dust transport and deposition towards the tropicalnorthern Atlantic. *Atmospheric Chemistry and Physics*, *9*(4), 1173–1189. https://doi.org/10.5194/acp-9-1173-2009

Stuut, J. B., Zabel, M., Ratmeyer, V., Helmke, P., Schefuß, E., Lavik, G., & Schneider, R. (2005). Provenance of present-day eolian dust collected off NW Africa. *Journal of Geophysical Research: Atmospheres*, *110*(4), 1–14. https://doi.org/10.1029/2004JD005161

Tesche, M., Ansmann, A., Müller, D., Althausen, D., Engelmann, R., Freudenthaler, V., & Groß, S. (2009). Vertically resolved separation of dust and smoke over Cape Verde using multiwavelength Raman and polarization lidars during Saharan Mineral Dust Experiment 2008. *Journal of Geophysical Research Atmospheres*, *114*(13), 1–14. https://doi.org/10.1029/2009JD011862

Tulet, P., Mallet, M., Pont, V., Pelon, J., & Boone, A. (2008). The 7-13 March 2006 dust storm over West Africa: Generation, transport, and vertical stratification. *Journal of Geophysical Research Atmospheres*, *113*(23), 1–13. https://doi.org/10.1029/2008JD009871

Wainker, D. M., Tackett, J. L., Getzewich, B. J., Liu, Z., Vaughan, M. A., & Rogers, R. R. (2013). The global 3-D distribution of tropospheric aerosols as characterized by CALIOP. *Atmospheric Chemistry and Physics*, *13*(6), 3345–3361. https://doi.org/10.5194/acp-13-3345-2013

Wandinger, U., Seifert, P., Engelmann, R., Bühl, J., Wagner, J., Schmidt, J., Pospichal, B., Baars, H., Hiebsch, A., Kanitz, T., Skupin, A., Pfitzenmaier, L., Heese, B., Althausen, D., & Ansmann, A. (2012). Observation of aerosol-cloud-turbulence interaction with integrated remote-sensing instrumentation. *Ninth International Symposium on Tropospheric Profiling*, *1*, 1–4. cetemps.aquila.infn.it/istp/proceedings/Session_C_Aerosols_clouds_and_precipitation/Session_C_Tuesday_4_September_2012/SC_02_Wandinger.pdf

Wang, W., Evan, A. T., Lavaysse, C., & Flamant, C. (2017). The role the Saharan Heat Low plays in dust emission and transport during summertime in North Africa. *Aeolian Research*, *28*, 1–12. https://doi.org/10.1016/j.aeolia.2017.07.001

Winker, D. M., Hunt, W. H., & McGill, M. J. (2007). Initial performance assessment of CALIOP. *Geophysical Research Letters*, *34*(19), 1–5. https://doi.org/10.1029/2007GL030135

Wurzler, S., Reisin, T. G., & Levin, Z. (2000). Modification of mineral dust particles by cloud processing and subsequent effects on drop size distributions. *Journal of Geophysical Research Atmospheres*, *105*(D4), 4501–4512. https://doi.org/10.1029/1999JD900980

Yu, H., Tan, Q., Chin, M., Remer, L. A., Kahn, R. A., Bian, H., Kim, D., Zhang, Z., Yuan, T., Omar, A. H., Winker, D. M., Levy, R. C., Kalashnikova, O., Crepeau, L., Capelle, V., & Chédin, A. (2019). Estimates of African Dust Deposition Along the Trans-Atlantic Transit Using the Decadelong Record of Aerosol Measurements from CALIOP, MODIS, MISR, and IASI. *Journal of Geophysical Research: Atmospheres*, *124*(14), 7975–7996. https://doi.org/10.1029/2019JD030574

Zipser, E. J., Twohy, C. H., Tsay, S. C., Thornhill, K. L., Tanelli, S., Ross, R., Krishnamurti, T. N., Ji, Q., Jenkins, G., Ismail, S., Hsu, N. C., Hood, R., Heymsfield, G. M., Heymsfield, A., Halverson, J., Goodman, H. M., Ferrare, R., Dunion, J. P., Douglas, M., … Anderson, B. (2009). The Saharan air layer and the fate of African easterly waves: NASA's AMMA field study of tropical cyclogenesis. *Bulletin of the American Meteorological Society*, *90*(8), 1137–1156. https://doi.org/10.1175/2009BAMS2728.1

Data availability

The CALIPSO data were obtained from the online archive of the ICARE Data and Services Center http://www.icare.univ-lille1.fr/archive (CALIPSO Science Team, 2015; ICARE Data Center, 2016. Reanalysis data are publicly available on the NASA Giovanni system (https://giovanni.sci.gsfc. nasa.gov/giovanni/). The LIVAS database is publicly available at http://lidar.space.noa.gr:8080/livas/. LIVAS EARLINET-optimized pure-dust products are available upon request from Eleni Marinou (elmarinou@noa.gr) and Vasilis Amiridis (vamoir@noa.gr).